LA-UR-12-00312

Approved for public release;
distribution is unlimited.

Title:	MCNP Geometry Transformation and Plotter Equations
Author(s):	Joe W. Durkee, Jr.
Intended for:	Publication in the journal Progress in Nuclear Energy

MCNP GEOMETRY TRANSFORMATION AND PLOTTER EQUATIONS

by

Joe W. Durkee, Jr.
Los Alamos National Laboratory
jdurkee@lanl.gov
505-665-0530
Fax: 505-665-2897
PO Box 1663, MS K575
Los Alamos, NM 87545

ABSTRACT

The MCNP Monte Carlo radiation-transport code contains versatile capabilities to develop and plot geometries used in simulations. Although these capabilities have been available in MCNP since the late 1970s, many of the derivational details underpinning these capabilities are not contained in the MCNP manual and do not appear to have been documented in Los Alamos reports or the published literature. Derivations of many of the equations underlying the MCNP geometry transformation and geometry plot utility are presented here. Although this document does not include derivations of all of the expressions contained in MCNP, its contents should nevertheless provide the reader with a deeper understanding of the geometry transformation and plotting features than can be obtained using only the MCNP theory manual.

KEYWORDS: MCNP; geometry; transformation; plot.

1. Introduction

Los Alamos National Laboratory (LANL) develops and maintains the MCNP (Brown, 2003) and, prior to the merger, the MCNPX™(Pelowitz, 2008) Monte Carlo N-Particle eXtended general-purpose radiation transport codes. We refer here primarily to MCNP because MCNP and MCNPX contain identical coding related to the subject matter contained in this document. Some specific mention of MCNPX is made here regarding the code identifier paradigm used in MCNPX but not in MCNP. A merged version of MCNP and MCNPX, MCNP6, is expected to be released in 2012. We refer here to MCNP in general except in instances where specific reference is made to a specific version of MCNP or to MCNPX.

MCNP accommodates intricate three-dimensional geometrical models, continuous-energy transport of 34 different particle types plus heavy-ion transport, fuel burnup, and high-fidelity delayed-gamma emission. MCNP is written in Fortran 90, has been parallelized, and works on platforms including single-processor personal computers (PCs), Sun workstations, Linux clusters, and supercomputers. MCNP has approximately 3000 users throughout the world working on endeavors that include radiation therapy, reactor design, and homeland security.

In the late 1970s the geometry treatment in MCNP was expanded and enhanced. The MCNP geometry transformation feature dates to the early 1980s (Thompson et. al, 1980), first appearing in MCNP 2B (Thompson, 1981). This feature provides the user with a

convienient and powerful means of specifying surfaces and objects to create problem geometry. This feature allows surfaces can be created in "local" coordinates, where their analytic-geometry definitions are simple, and then be moved via translation and/or rotation operations to their desired "global-coordinate" locations. Beginning with MCNP 2B, the code has possessed the ability to treat geometry transformation using the coordinate transformation TR card as described in the Coordinate Transformation Card section of the user's manuals. In that section, the displacement ("O") and rotation ("B") elements of a geometry transformation are described and their use illustrated. However, it appears that no documentation exists that explains the derivation of the coordinate transformation feature.

Visualization of model geometry and of calculated results ("tallies") is an important component of the simulation process, particularly when complex models involving multi-particle transport are being analyzed. Since its creation three decades ago, the MCNP interactive "PLOT" package has been used to plot model geometry. The "MCPLOT" package has been used to make two-dimensional (2-D) plots of tally information (i.e., calculated fluxes, currents, etc.) and of nuclear cross-section data.

Chapter 2 of the MCNP (Thompson, 1979), MCNP4A (Breismeister, 1993), and MCNP5 (Brown, 2003a) manuals gives some description and derivational information about the geometry plotter and how it draws cross-sectional views of the problem geometry. Included is information discussing the intersection of three-dimensional (3-D) surfaces with the plot plane and how the surfaces are expressed in plot-plane (s,t)

coordinates. Comments and expressions for a set of one-parameter equations for the surfaces in the plot plane are then provided without derivation.

In this paper many of the expressions for the geometry transformation and plotting features are derived. Although the geometry transformation derivation is straightforward, we will point out an important coding nuance that should be carefully noted by code developers. The derivation of the plotter equations is not necessary straightforward, and the derivation of all coded expressions is very lengthy. As such, we present derivations for an illustrative, yet substantive subset of the cases that have been coded. Included in the plotter derivation are the one-parameter ("*p*") expressions. It is these expressions that permit plotting of curves in a straightforward manner that is visually appealing, facilitate the checking whether a surface is within the extent of the plot window, and enable the checking of the sense with respect to cells bounded by a particular surface. The derivation of these single-parameter expressions appears not to have previously been documented in detail. Because they are central to the PLOT package, they are documented here. During our discussion, specific subroutines and code lines will be highlighted to help tie the derivations and coding together.

We cite the work of Thomas N. K. Godfrey in developing the geometry translation and rotation capability for MCNP (Thompson et al., 1980; Thompson, 1981). We also acknowledge the work that William M. Taylor and Charles A. Forest performed in the

1970's to develop the geometry plotting capability.[†] They drew in part from Spain (2007), a fresh print of which has recently been released by Dover Publications.

During the derivation of the geometry transformation equations, it was discovered that the theoretical equations differed from the coded expressions in subroutines **trfsrf.F**, **dunlev.F**, etc. In particular, the rotation-component "B" values in the TRF matrix are transposed relative to the theoretical representation. MCNP corrects this difference via the transpose operation performed in subroutine **trfsrf.F** during processing of the input data. Thus, in effect, MCNP transposes the TRF matrix twice to perform the correct coordinate-transformation operation. This matter is discussed in detail in Section 3.

2. Overview of geometry transformation and plotting code flow.

The general flow for the geometry transformation and plotting treatment follows. The reader should also consult the MCNP manuals (Thompson, 1979; Breismeister, 1993; Brown, 2003a).

Geometry transformations involve individual surfaces (e.g., planes, spheres, etc.) or macrobodies (e.g., RPP, RCC, etc.) that are specified in "auxiliary" coordinates (x', y', z'). This convention simplifies specification for objects whose orientation is not parallel to one of the global-coordinate axes. Specifications for a surface's geometry translation and/or rotation are input using the TR card. MCNP uses this transformation to

[†] Personal communication from John S. Hendricks June 17, 2010 regarding their undocumented contributions. Dr. Hendricks states that name choices of many of the PLOT subroutines were selected by Charles Forest to reflect his appreciation of Latin.

locate and orient each surface in (x, y, z), and subsequently uses the global-coordinate surfaces to do radiation transport and geometry plotting.

MCNP performs geometry plotting by first finding the intersection of each global-coordinate surface with the plot plane. This requires a transformation from (x, y, z) coordinates to (*s*,*t*) plot-plane coordinates. This transformation is transparent to the user (i.e., no input is required).

The bivariate plot-plane surface intersection equations (line, parabola, hyperbola, ellipse) are then transformed to a univariate (*p*) representation. In this form, points of intersection (POIs) for surfaces in the plot plane are determined. MCNP then identifies the cells on either side of a line between each POI. Use of the univariate representation simplifies these tasks as compared to using the bivariate formulation.

The terminology "auxiliary" and (x, y, z) coordinates is historical. In the following discussion, we use "local" (or object) coordinates[†] (x^L, y^L, z^L) instead of auxiliary coordinates and "global" coordinates $\left(x^G, y^G, z^G\right)$ instead of (x, y, z) coordinates.

Using this updated terminology, the general geometry and plotting code flow is sketched in Fig. 1.

[†] Termed "auxiliary" coordinates (x', y', z') in the theory and user's manuals.

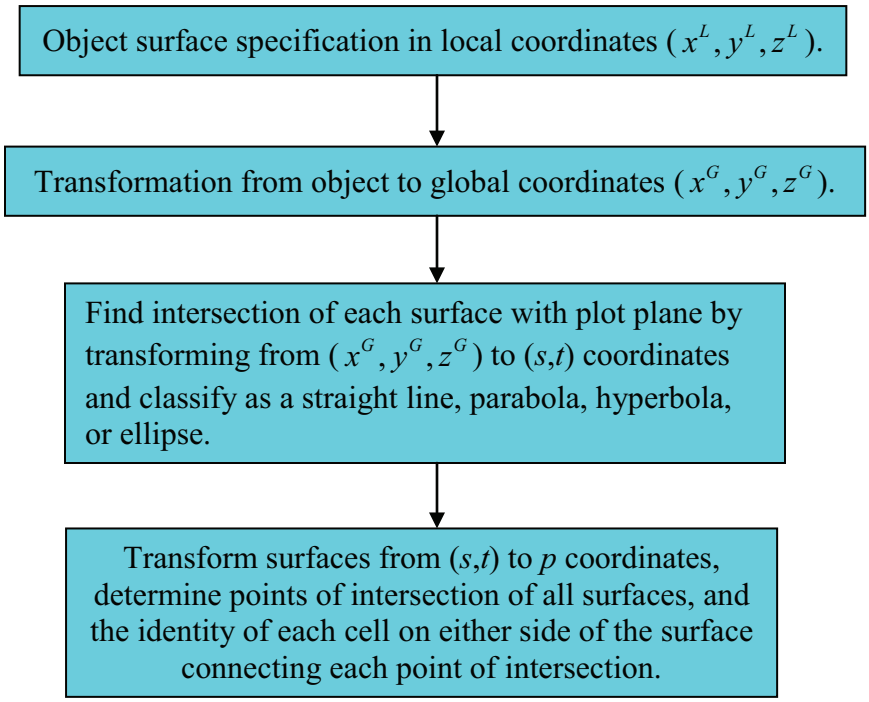

Figure 1. General geometry transformation and plotting code flow for geometry transformation.

3. Geometry transformation.

MCNP represents 3-D surfaces using quadratic and matrix representations. Matrix expressions are used to perform geometry transformations. MCNP requires that all surfaces be represented in global coordinates (x^G, y^G, z^G). It offers the user the ability to represent surfaces in local coordinates (x^L, y^L, z^L) and then perform translation and/or rotation operations to move each surface to global coordinates.

The equation of a surface in MCNP can be written as a general quadratic of the form (Brown, 2003a; Spain, 2007; Tierney, 1974)

$$Ax^2 + By^2 + Cz^2 + Dxy + Eyz + Fzx + Gx + Hy + Jz + K = 0\,. \tag{1}$$

In matrix form, Eq.(1) becomes

$$\begin{bmatrix} 1 & x & y & x \end{bmatrix} AM \begin{bmatrix} 1 \\ x \\ y \\ z \end{bmatrix} = 0 \tag{2}$$

where the AM matrix is

$$AM = \begin{bmatrix} K & G/2 & H/2 & J/2 \\ G/2 & A & D/2 & F/2 \\ H/2 & D/2 & B & E/2 \\ J/2 & F/2 & E/2 & C \end{bmatrix}. \tag{3}$$

Equations (1)–(3) are valid for surfaces in local and global coordinates. Thus, the matrix representation for local coordinates is

$$\begin{bmatrix} 1 & x^L & y^L & x^L \end{bmatrix} AM^L \begin{bmatrix} 1 \\ x^L \\ y^L \\ z^L \end{bmatrix} = 0\,, \tag{4}$$

while for global coordinates it is

$$\begin{bmatrix} 1 & x^G & y^G & x^G \end{bmatrix} AM^G \begin{bmatrix} 1 \\ x^G \\ y^G \\ z^G \end{bmatrix} = 0\,. \tag{5}$$

The local-coordinate representation of a surface is related to the global-coordinate representation via the transformation

$$\begin{bmatrix} 1 \\ x^L \\ y^L \\ z^L \end{bmatrix} = TRF \begin{bmatrix} 1 \\ x^G \\ y^G \\ z^G \end{bmatrix} \tag{6}$$

where *TRF* is the transformation matrix. We will consider the contents of *TRF* shortly.

Taking the transpose of Eq.(6) gives

$$\begin{bmatrix} 1 & x^L & y^L & z^L \end{bmatrix} = \begin{bmatrix} 1 & x^G & y^G & z^G \end{bmatrix} TRF^T . \tag{7}$$

Substituting Eqs.(6) and (7) into Eq.(4) gives

$$\begin{bmatrix} 1 & x^G & y^G & x^G \end{bmatrix} TRF^T AM^L TRF \begin{bmatrix} 1 \\ x^G \\ y^G \\ z^G \end{bmatrix} = 0 , \tag{8}$$

which is the global-coordinate matrix form for a surface given its local-coordinate coefficients in the AM^L matrix and the transformation matrix *TRF*. We may now write Eq.(5) with AM^G given by

$$AM^G = TRF^T AM^L TRF . \tag{9}$$

The calculation of Eq.(9) is performed in subroutine **trfsrf.F**, lines ss.18-ss.27.[†] First, the "TM" matrix in **trfsrf.F** is used to store the *TRF* transformation-matrix contents. Then, the local-coordinate surface-coefficient matrix AM^L is loaded in subroutine **amatrx.F** using the general-quadratic surface-coefficient "SCF" array values input by the user via the cell cards.[*] Next, two calls are made to subroutine **matmpy.F** to perform the matrix-multiplication operations in Eq.(9) to obtain the global-coordinate surface coefficient matrix AM^G. After some manipulations, the global-coordinate surface coefficients are loaded into the SCF array in lines ss.130-ss.131 in **trfsrf.F**. These SCF values are used for particle tracking and geometry plotting.

[†] As mentioned, code line identifiers pertain to MCNPX.
[*] Input in subroutine **oldcrd.F**.

According to subroutine **trfsrf.F**, lines ss.18-ss.21, the *TRF* contents (more precisely, the TM array values) are given by

$$TRF = \begin{bmatrix} 1 & 0 & 0 & 0 \\ \Delta x^G & B_1^{GL} & B_4^{GL} & B_7^{GL} \\ \Delta y^G & B_2^{GL} & B_5^{GL} & B_8^{GL} \\ \Delta z^G & B_3^{GL} & B_6^{GL} & B_9^{GL} \end{bmatrix}, \tag{10}$$

where the *B*s are defined in the theory manual (Brown, 2003b) as

$$\begin{aligned} B_1^{GL} &= \hat{i}^G \cdot \hat{i}^L, \quad B_2^{GL} = \hat{j}^G \cdot \hat{i}^L, \quad B_3^{GL} = \hat{k}^G \cdot \hat{i}^L \\ B_4^{GL} &= \hat{i}^G \cdot \hat{j}^L, \quad B_5^{GL} = \hat{j}^G \cdot \hat{j}^L, \quad B_6^{GL} = \hat{k}^G \cdot \hat{j}^L \\ B_7^{GL} &= \hat{i}^G \cdot \hat{k}^L, \quad B_8^{GL} = \hat{j}^G \cdot \hat{k}^L, \quad B_9^{GL} = \hat{k}^G \cdot \hat{k}^L . \end{aligned} \tag{11}$$

Let us examine the rotation elements more closely. Using Eq.(10) in Eq.(6) gives

$$\begin{aligned} x^L &= \Delta x^G + B_1^{GL} x^G + B_4^{GL} y^G + B_7^{GL} z^G \\ y^L &= \Delta y^G + B_2^{GL} x^G + B_5^{GL} y^G + B_8^{GL} z^G \\ z^L &= \Delta z^G + B_3^{GL} x^G + B_6^{GL} y^G + B_9^{GL} z^G \end{aligned} \tag{12}$$

which, using the definitions of the *B*s from Eq.(11), becomes

$$\begin{aligned} x^L &= \Delta x^G + \hat{i}^G \cdot \hat{i}^L x^G + \hat{i}^G \cdot \hat{j}^L y^G + \hat{i}^G \cdot \hat{k}^L z^G \\ y^L &= \Delta y^G + \hat{j}^G \cdot \hat{i}^L x^G + \hat{j}^G \cdot \hat{j}^L y^G + \hat{j}^G \cdot \hat{k}^L z^G \\ z^L &= \Delta z^G + \hat{k}^G \cdot \hat{i}^L x^G + \hat{k}^G \cdot \hat{j}^L y^G + \hat{k}^G \cdot \hat{k}^L z^G \end{aligned} . \tag{13}$$

This expression does <u>not</u> reduce to a form that represents the projection of the position vector $\vec{R}^G = x^G \hat{i}^G + y^G \hat{j}^G + z^G \hat{k}^G$ onto the local-coordinate unit vectors $\hat{i}^L$, $\hat{j}^L$, and $\hat{k}^L$. This puzzling fact hints that the form of *TRF* in Eq.(10) and in **trfsrf.F** is questionable.

Now let us consider coordinate rotation as illustrated by the two rectangular coordinate systems shown in Fig. 2. Because the origins of the two coordinates systems

are identical, this configuration depicts coordinate rotation and excludes coordinate translation.

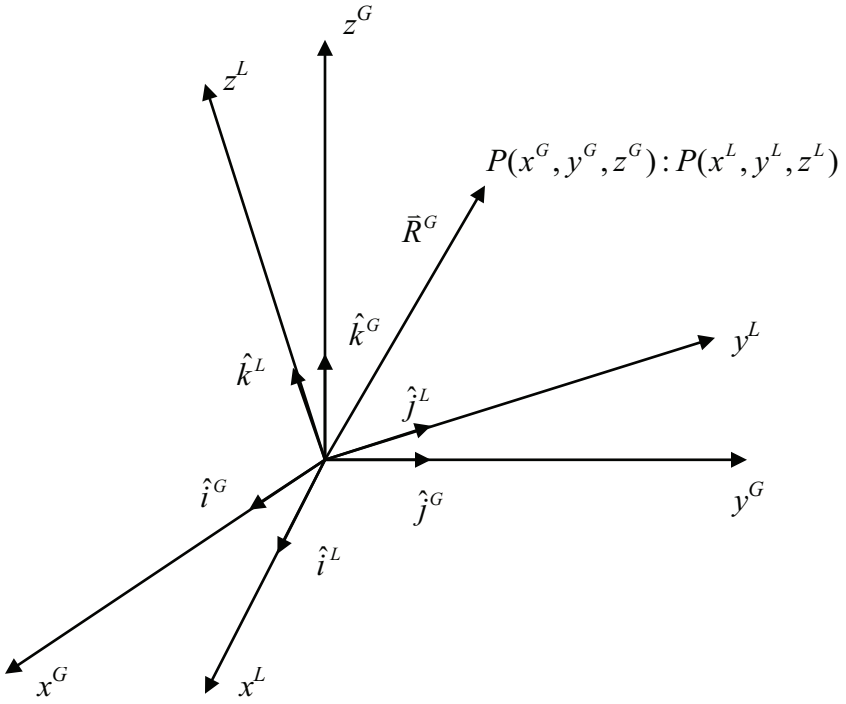

Figure 2. Coordinate-system rotation illustrated by global and local rectangular coordinate systems having the same origin.

The values of the local-coordinate variables x^L, y^L, z^L can be obtained by projecting the position vector $\vec{R}^G$ onto the local-coordinate unit vectors $\hat{i}^L$, $\hat{j}^L$, and $\hat{k}^L$ (Wylie, 1975). Thus,

$$\begin{aligned} x^L &= \Delta x^G + \hat{i}^G \cdot \hat{i}^L x^G + \hat{j}^G \cdot \hat{i}^L y^G + \hat{k}^G \cdot \hat{i}^L z^G = \Delta x^G + \vec{R}^G \cdot \hat{i}^L \\ y^L &= \Delta y^G + \hat{i}^G \cdot \hat{j}^L x^G + \hat{j}^G \cdot \hat{j}^L y^G + \hat{k}^G \cdot \hat{j}^L z^G = \Delta y^G + \vec{R}^G \cdot \hat{j}^L , \\ z^L &= \Delta z^G + \hat{i}^G \cdot \hat{k}^L x^G + \hat{j}^G \cdot \hat{k}^L y^G + \hat{k}^G \cdot \hat{k}^L z^G = \Delta z^G + \vec{R}^G \cdot \hat{k}^L \end{aligned} \qquad (14)$$

where

$$\vec{R}^G = x^G \hat{i}^G + y^G \hat{j}^G + z^G \hat{k}^G \,. \tag{15}$$

Using the MCNP definitions for $B_1^{GL} - B_9^{GL}$ from Eq.(11), Eq.(14) becomes

$$\begin{aligned} x^L &= \Delta x^G + B_1^{GL} x^G + B_2^{GL} y^G + B_3^{GL} z^G \\ y^L &= \Delta y^G + B_4^{GL} x^G + B_5^{GL} y^G + B_6^{GL} z^G \\ z^L &= \Delta z^G + B_7^{GL} x^G + B_8^{GL} y^G + B_9^{GL} z^G \end{aligned} \,. \tag{16}$$

Consequently, the transformation matrix $T\tilde{R}F$ takes the form

$$T\tilde{R}F = \begin{bmatrix} 1 & 0 & 0 & 0 \\ \Delta x^G & B_1^{GL} & B_2^{GL} & B_3^{GL} \\ \Delta y^G & B_4^{GL} & B_5^{GL} & B_6^{GL} \\ \Delta z^G & B_7^{GL} & B_8^{GL} & B_9^{GL} \end{bmatrix}. \tag{17}$$

Comparing Eq.(17), the rotation-matrix elements derived by projecting the position vector $\vec{R}^G$ onto the local-coordinate unit vectors, to Eq.(10), the MCNP rotation matrix, reveals that the rotation components of *TRF* and $T\tilde{R}F$ are transposed.

The key operation involving the transformation matrix *TRF* appears in Eq.(8). If the version of *TRF* in Eq.(10) (and coded in **trfsrf.F**) were a typo, and if the version in Eq.(17) is the actual transformation matrix, then matters would "work out" if

$$TRF^T \, AM^L \, TRF = TRF \, AM^L \, TRF^T \,. \tag{18}$$

Unfortunately, even though *AM* is symmetric as seen in Eq.(3),

$$TRF^T \, AM^L \, TRF \neq TRF \, AM^L \, TRF^T \,. \tag{19}$$

This draws into question the meaning of the rotation-matrix elements in MCNP.

The conflict is resolved in MCNP as follows. The *B*s from TR cards are input into **nextit.F** during **rdprob.F** processing. Subroutine **rdprob.F** then calls **oldcrd.F**, which calls **trfmat.F**. Subroutine **trfmat.F** does several things, including orthonormalizing and transposing the *B*s (*TRF* matrix) in lines tm4b.15-tm.112. The coding in subroutine **trfsrf.F**, lines ss.18-ss.21, transposes the *B*s so that the matrix appears as in Eq.(17) rather than Eq.(10). Thus, MCNP is performing properly, albeit with two (seemingly unnecessary) transpose operations.

4. Geometry plotter: intersection of 3-D surfaces with the plot plane.

The MCNP geometry plotter draws cross-sectional views of the problem geometry according to commands entered by the user. MCNP determines the intersection of each global-coordinate surface with the plot plane. The expressions in the MCNP manuals and the derivation of these expressions rely on analytic geometry and matrix theory for linear and quadratic algebraic equations.

From Eq.(1), the equation of an MCNP global-coordinate surface is

$$\begin{aligned} &A^G(x^G)^2 + B^G(y^G)^2 + C^G(z^G)^2 + D^G x^G y^G + E^G y^G z^G + F^G x^G z^G \\ &+G^G x^G + H^G y^G + J^G z^G + K^G = 0 \quad . \end{aligned} \tag{20}$$

The surface coefficients $A^G - K^G$ are contained in the SCF array as loaded in **trfsrf.F** lines ss.130–ss.131.

The equation of the plot plane can be expressed using the parametric representation for the equation of a plane (Trench, 1972). The plot plane is specified in terms of its position with respect to the origin and the orientation of its coordinate axes with respect

to the surfaces of the problem. The position of the plot plane with respect to the origin is given by the vector $\vec{r}_0$. The plot plane is characterized by two linearly independent basis vectors $\vec{a}$ and $\vec{b}$ and the parameters *s* and *t* so that

$$\vec{r} = \vec{r}_0 + s\vec{a} + t\vec{b} \tag{21}$$

where

$$\begin{aligned} \vec{r} &= x\hat{i} + y\hat{j} + z\hat{k} \\ \vec{r}_0 &= x_0\hat{i} + y_0\hat{j} + z_0\hat{k} \\ \vec{a} &= a_x\hat{i} + a_y\hat{j} + a_z\hat{k} \\ \vec{b} &= b_x\hat{i} + b_y\hat{j} + b_z\hat{k} \quad . \end{aligned} \tag{22}$$

Figure 3 illustrates the plot plane and an object intersecting the plane.

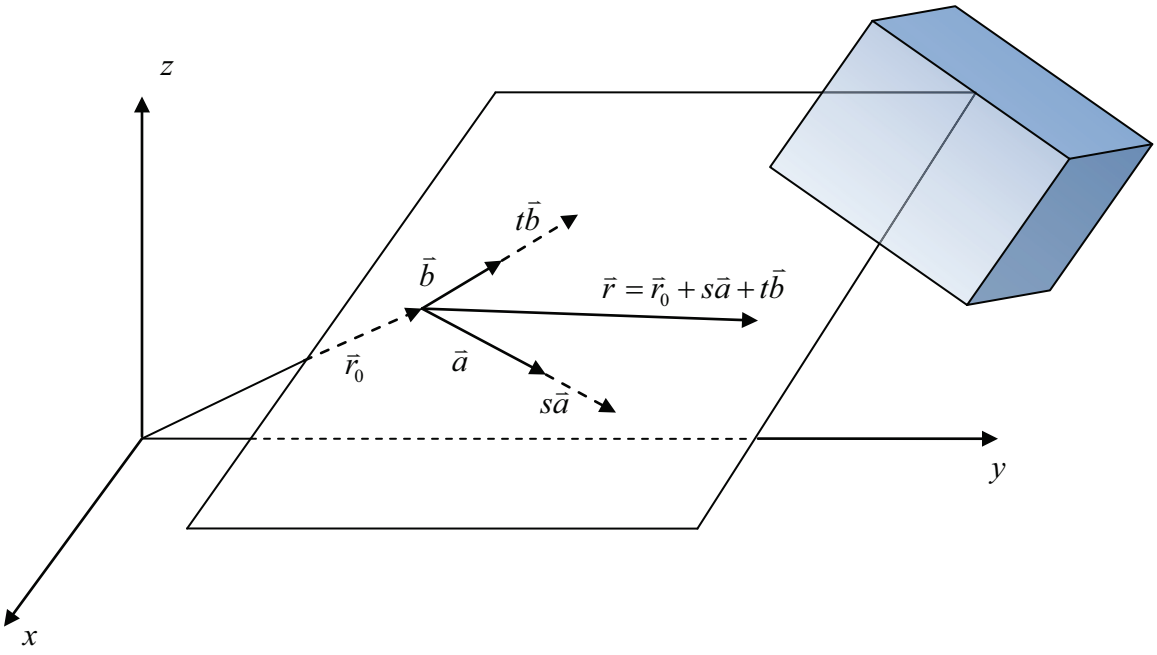

Figure 3. Plot plane and rectangular object.

In matrix form Eqs.(21) and (22) are

$$\begin{bmatrix} 1 \\ x^G \\ y^G \\ z^G \end{bmatrix} = \begin{bmatrix} 1 & 0 & 0 \\ x_0 & a_x & b_x \\ y_0 & a_y & b_y \\ z_0 & a_z & b_z \end{bmatrix} \begin{bmatrix} 1 \\ s \\ t \end{bmatrix} = PL \begin{bmatrix} 1 \\ s \\ t \end{bmatrix} \tag{23}$$

where

$$PL = \begin{bmatrix} 1 & 0 & 0 \\ x_0 & a_x & b_x \\ y_0 & a_y & b_y \\ z_0 & a_z & b_z \end{bmatrix}. \tag{24}$$

We seek to develop the expression for intersection of a 3-D surface with the plot plane. It can be shown that, with the exception of two parallel lines, the intersection of a plane and a 3-D surface can be written as general bivariate quadratic (Hsiung and Mao, 1998; Kwak and Hong, 1997; Spain, 2007; Tierney, 1974, p.230) in the form (Spain, 2007)

$$A^P s^2 + 2H^P st + B^P t^2 + 2G^P s + 2F^P t + C^P = 0 \tag{25}$$

using the plot-plane coordinate variables *s* and *t*. The superscript "*P*" is used here to explicitly connote that these coefficients pertain to the plot-plane conic rather than the coefficients of the surface intersecting the plot plane. This is the representation of a conic in the plot plane that is used in MCNP (Brown, 2003a). In matrix form Eq.(25) is

$$\begin{bmatrix} 1 & s & t \end{bmatrix} \begin{bmatrix} C^P & G^P & F^P \\ G^P & A^P & H^P \\ F^P & H^P & B^P \end{bmatrix} \begin{bmatrix} 1 \\ s \\ t \end{bmatrix} = \begin{bmatrix} 1 & s & t \end{bmatrix} QM \begin{bmatrix} 1 \\ s \\ t \end{bmatrix} = 0. \tag{26}$$

Taking the transpose of Eq.(23)

$$\begin{bmatrix} 1 & x^G & y^G & z^G \end{bmatrix} = \begin{bmatrix} 1 & s & t \end{bmatrix} PL^T \tag{27}$$

and substituting into Eq.(2) gives the equation of a 3-D object in terms of plot-plane coordinates:

$$\begin{bmatrix} 1 & s & t \end{bmatrix} PL^T AM^G \; PL \begin{bmatrix} 1 \\ s \\ t \end{bmatrix} = 0 . \tag{28}$$

Comparison of Eq.(28) and Eq.(26) shows that

$$QM = PL^T AM^G \; PL = \begin{bmatrix} C^P & G^P & F^P \\ G^P & A^P & H^P \\ F^P & H^P & B^P \end{bmatrix} \equiv \begin{bmatrix} q_{11} & q_{12} & q_{13} \\ q_{21} & q_{22} & q_{23} \\ q_{31} & q_{32} & q_{33} \end{bmatrix} . \tag{29}$$

Inspection of Eq.(29) shows the QM matrix is both square and symmetric, i.e.,

$$QM = PL^T AM^G \; PL = \begin{bmatrix} C^P & G^P & F^P \\ G^P & A^P & H^P \\ F^P & H^P & B^P \end{bmatrix} \equiv \begin{bmatrix} q_{11} & q_{12} & q_{13} \\ q_{12} & q_{22} & q_{23} \\ q_{13} & q_{23} & q_{33} \end{bmatrix} . \tag{30}$$

Equation (28) can thus be written as

$$\begin{bmatrix} 1 & s & t \end{bmatrix} QM \begin{bmatrix} 1 \\ s \\ t \end{bmatrix} = 0 , \tag{31}$$

or in the quadratic form

$$q_{22}s^2 + 2q_{23}st + q_{33}t^2 + 2q_{12}s + 2q_{13}t + q_{11} = 0 . \tag{32}$$

Eq. (31) gives the matrix form of the expression for the intersection of a 3-D surface with the plot plane, i.e., the curve(s) to be plotted. The QM matrix is a matrix of the coefficients for the quadratic form of the surface(s) in the plot plane. However, these

expressions contain two plot variables *s* and *t*. The question arises how to select the values of *s* and *t* so that an adequate series of points along the curve(s) can be selected and plotted using piecewise linear line segments between the points. As pointed out in the 1979 MCNP manual (Thompson, 1979), there is no consistent way to generate the sets of points that lie on the curve for a two-parameter expression. Instead of a two-parameter expression, we need a one-parameter representation of Eq.(31) such that, for the parameter *p*,

$$s = s(p), t = t(p), -\infty \le p \le \infty . \tag{33}$$

To develop a one-parameter expression, some useful properties of equations and matrices are used.

Recall that the MCNP geometry-transformation feature (Section 3) takes advantage of the simplicity with which surfaces can be defined in local coordinates. These surfaces can be translated and rotated to their general-coordinate locations and used to form objects with desired locations and orientations. This notion is used for the plotter equations, but in a reverse sense: equations can have simpler forms if they are translated and/or rotated to other coordinate systems (Kwak and Hong, 1997; Tierney, 1974 pp. 204–206, 225–226). We seek to simplify Eq.(31) by translation and/or rotation operations to obtain the simplest form of the general quadratic equation in an alternate coordinate system.

Before considering the translation/rotation matrix, we consider some useful properties from matrix theory. First, recall that an "elementary transformation" of a matrix is any one of the following operations (Wylie, p. 491):

a. The multiplication of each element of a row or a column by the same nonzero constant.
b. The interchange of two rows or of two columns.
c. The addition of any multiple of the elements of one row, or one column, to the corresponding elements of another row, or column, respectively.

Second, two matrices are "equivalent" if either of these matrices can be obtained from the other by a series of elementary transformations (Wylie, p. 493). Third, a theorem of matrix theory is that if A and B are equivalent matrices, then $B = PAQ$, where P and Q are nonsingular matrices (Wylie, p. 493). Fourth, a theorem of matrix theory is that any square matrix is equivalent to a diagonal matrix (Wylie, p. 494). Fifth, a theorem of matrix theory is that a square matrix is congruent (has the same size and shape) to a diagonal matrix if and only if it is symmetric, that is $B = Q^T AQ$ (Hsiung and Mao, p. 150; Wylie, p. 549).

These definitions and theorems are used for the MCNP plotter. Because QM matrix is both square and symmetric, Eq.(30), a single matrix DIA and its transpose[†] can be used to perform congruence transform (Wylie, p. 497) with the property that $DIA^T QM\ DIA$ is diagonal (Wylie, p. 549).

[†] Rather than two nonsingular matrices for a general equivalence transformation.

The matrix to be used to effect the congruence transformation and change Eq.(32) into its simplest form is the general translation and rotation operation matrix in the plot plane, defined in the *u*-*v* coordinate system (Thompson, 1979; Spain, 2007 pp. 62–64; Tierney, 1974 pp. 204–206, 225–226) [†]

$$\begin{bmatrix} 1 \\ s \\ t \end{bmatrix} = \begin{bmatrix} 1 & 0 & 0 \\ s_0 & \cos\theta & -\sin\theta \\ t_0 & \sin\theta & \cos\theta \end{bmatrix} \begin{bmatrix} 1 \\ u \\ v \end{bmatrix} \tag{34}$$

or

$$\begin{bmatrix} 1 \\ s \\ t \end{bmatrix} = DIA \begin{bmatrix} 1 \\ u \\ v \end{bmatrix}, \tag{35}$$

where

$$DIA = \begin{bmatrix} 1 & 0 & 0 \\ s_0 & \cos\theta & -\sin\theta \\ t_0 & \sin\theta & \cos\theta \end{bmatrix}. \tag{36}$$

The *DIAG* matrix is

$$DIAG = DIA^T QM\ DIA = \begin{bmatrix} d_{11} & d_{12} & d_{13} \\ d_{21} & d_{22} & d_{23} \\ d_{31} & d_{32} & d_{33} \end{bmatrix}, \tag{37}$$

where

[†] The important details in Eqs.(34)–(37) are omitted from subsequent MCNP manuals.

$$
\begin{aligned}
d_{11} &= q_{11} + (q_{12} + q_{21})s_0 + q_{22}s_0^2 + (q_{13} + q_{31})t_0 + (q_{23} + q_{32})s_0t_0 + q_{33}t_0^2 \\
d_{12} &= \cos\theta\left(q_{12} + q_{22}s_0 + q_{32}t_0\right) + \sin\theta\left(q_{13} + q_{23}s_0 + q_{33}t_0\right) \\
d_{21} &= \cos\theta\left(q_{21} + q_{22}s_0 + q_{23}t_0\right) + \sin\theta\left(q_{31} + q_{32}s_0 + q_{33}t_0\right) \\
d_{13} &= -\sin\theta\left(q_{12} + q_{22}s_0 + q_{32}t_0\right) + \cos\theta\left(q_{13} + q_{23}s_0 + q_{33}t_0\right) \\
d_{31} &= -\sin\theta\left(q_{21} + q_{22}s_0 + q_{23}t_0\right) + \cos\theta\left(q_{31} + q_{23}s_0 + q_{33}t_0\right) \\
d_{23} &= \cos\theta\left(q_{23}\cos\theta - q_{22}\sin\theta\right) + \sin\theta\left(q_{33}\cos\theta - q_{32}\sin\theta\right) \\
d_{32} &= \cos\theta\left(q_{32}\cos\theta - q_{22}\sin\theta\right) + \sin\theta\left(q_{33}\cos\theta - q_{23}\sin\theta\right) \\
d_{22} &= \cos\theta\left(q_{22}\cos\theta + q_{23}\sin\theta\right) + \sin\theta\left(q_{23}\cos\theta + q_{33}\sin\theta\right) \\
d_{33} &= -\sin\theta\left(q_{23}\cos\theta - q_{22}\sin\theta\right) + \cos\theta\left(q_{33}\cos\theta - q_{23}\sin\theta\right) \quad .
\end{aligned}
\tag{38}
$$

From Eq.(30), symmetry of the QM matrix means that $d_{ij} = d_{ji}$ so that

$$
DIAG = DIA^T QM\ DIA = \begin{bmatrix} d_{11} & d_{12} & d_{13} \\ d_{12} & d_{22} & d_{23} \\ d_{13} & d_{23} & d_{33} \end{bmatrix}, \tag{39}
$$

with d_{11} simplifying to

$$
d_{11} = q_{11} + 2q_{12}s_0 + q_{22}s_0^2 + 2q_{13}t_0 + 2q_{23}s_0t_0 + q_{33}t_0^2 . \tag{40}
$$

Writing the intersection of an MCNP surface with the plot plane as "*I*," we take Eq.(26) and use Eq.(35) to give the intersection of a surface and the plot plane in (u, v) as

$$
I = \begin{bmatrix} 1 & u & v \end{bmatrix} DIA^T QM\ DIA \begin{bmatrix} 1 \\ u \\ v \end{bmatrix} = 0 . \tag{41}
$$

Using Eq.(39), Eq.(41) expands to

$$
I = d_{11} + 2d_{12}u + 2d_{13}v + 2d_{23}uv + d_{22}u^2 + d_{33}v^2 = 0 . \tag{42}
$$

Equation (42) has the same form as Eq.(25); thus, Eq.(42) is a general bivariate quadratic.

The parameters of the transform, s_0, t_0, and θ are determined so that

the *uv* term is eliminated from Eq.(42) to give

$$I^D = d_{11}^D + 2d_{12}^D u + 2d_{13}^D v + d_{22}^D u^2 + d_{33}^D v^2 = 0\,. \tag{43}$$

Specific forms of Eq.(43) are obtained depending on the type of curve (conic) that is produced by the intersection of the 3-D surface with the plot plane. The diagonalization of the *QM* matrix thus introduces a coordinate system in u and v in which the equations of the conic sections have their simplest and most symmetric form. The one-parameter set of relationships is of the form $u = u(p)$ and $v = v(p)$, where $-\infty \le p \le \infty$. Using the transformation Eq.(36), we can then obtain $s = s(p)$ and $t = t(p)$.

For use with curves in the plot plane other than straight lines, Eq.(43) is obtained as follows. There exists an angle θ^D, satisfying $0 < \theta^D < \pi/2$, such that a rotation of the quadratic surface through θ^D will cause $d_{23}^D = 0$ and thereby eliminate term in *uv* from Eq.(42).[†] The expression for d_{23} in Eq.(38) contains only the angle θ (not s_0 or t_0), so we can solve $d_{23}^D = 0$ for the angle:

$$\begin{aligned} \cos\theta\left(q_{23}\cos\theta - q_{22}\sin\theta\right) + \sin\theta\left(q_{33}\cos\theta - q_{23}\sin\theta\right) &= 0 \\ q_{23}\left(\cos^2\theta - \sin^2\theta\right) + \left(q_{33} - q_{22}\right)\cos\theta\sin\theta &= 0 \\ q_{23}\cos 2\theta + \frac{1}{2}\left(q_{33} - q_{22}\right)\sin 2\theta &= 0 \end{aligned} \tag{44}$$

so that the rotation angle θ^D which satisfies the diagonalization condition is

$$\theta^D = \frac{1}{2}\tan^{-1}\left(\frac{2q_{23}}{q_{22} - q_{33}}\right). \tag{45}$$

[†] This property is also a mathematical theorem (Tierney, 1974 p. 227).

Equation (45) is coded in subroutine **regula.F** statement rg.67 for use with surfaces in the plot plane other than straight lines.

To recap, the equation for the intersection of an MCNP surface given by Eq.(20) with the plot plane is a conic given by Eq.(25). The equation for this conic can be written in matrix form given by Eq.(26). This bivariate expression can be recast as a univariate expression by the use of a general translation and rotation operation in the plot plane as given by Eqs.(35) and (36). The univariate expression is suitable for plotting purposes.

We will use the diagonalization condition in Eq.(39) with a determination of the transform parameters s_0, t_0, and θ to obtain the conditions that cause $I^D = 0$ in Eq.(43) for four types of conics in the plot plane. First we will treat cases where a plane and a sphere intersect the plot plane. The intersection of a plane with the plot plane produces a line, whereas a sphere creates a circle, ellipse, or a point. The intersection of other types of surfaces with the plot plane causing a hyperbola or a parabola will then be examined.

4.1. Intersection of a plane with the plot plane

To illustrate the procedure for developing a one-parameter expression for a 3-D surface in the plot plane, let us consider the 3-D surface to be a plane. Intuitively, the intersection will be a line. For a plane, Eq.(20) becomes

$$G^G x^G + H^G y^G + J^G z^G + K^G = 0, \tag{46}$$

so that the matrix representation given by Eq.(5),

$$\begin{bmatrix} 1 & x^G & y^G & x^G \end{bmatrix} AM^G \begin{bmatrix} 1 \\ x^G \\ y^G \\ z^G \end{bmatrix} = 0\,, \tag{47}$$

has the coefficient matrix given by Eq. (3) written as

$$AM^G = \begin{bmatrix} K^G & G^G/2 & H^G/2 & J^G/2 \\ G^G/2 & 0 & 0 & 0 \\ H^G/2 & 0 & 0 & 0 \\ J^G/2 & 0 & 0 & 0 \end{bmatrix}. \tag{48}$$

The expression for the plane in plot-plane coordinates is given by Eq.(31) with

$$QM = \begin{bmatrix} K^G + G^G x_0 + H^G y_0 + J^G z_0 & \frac{a_x G^G}{2} + \frac{a_y H^G}{2} + \frac{a_z J^G}{2} & \frac{b_x G^G}{2} + \frac{b_y H^G}{2} + \frac{b_z J^G}{2} \\ \frac{a_x G^G}{2} + \frac{a_y H^G}{2} + \frac{a_z J^G}{2} & 0 & 0 \\ \frac{b_x G^G}{2} + \frac{b_y H^G}{2} + \frac{b_z J^G}{2} & 0 & 0 \end{bmatrix} \tag{49}$$

or

$$QM = \begin{bmatrix} q_{11} & q_{12} & q_{13} \\ q_{21} & 0 & 0 \\ q_{31} & 0 & 0 \end{bmatrix} \tag{50}$$

or, noting the symmetry,

$$QM = \begin{bmatrix} q_{11} & q_{12} & q_{13} \\ q_{12} & 0 & 0 \\ q_{13} & 0 & 0 \end{bmatrix} \tag{51}$$

where

$$
\begin{aligned}
q_{11} &= K^G + G^G x_0 + H^G y_0 + J^G z_0 \\
q_{12} &= \frac{a_x G^G}{2} + \frac{a_y H^G}{2} + \frac{a_z J^G}{2} \\
q_{13} &= \frac{b_x G^G}{2} + \frac{b_y H^G}{2} + \frac{b_z J^G}{2} \quad .
\end{aligned} \tag{52}
$$

We next seek to formulate and solve Eq.(41) for the case of a plane intersecting the plot plane. First, the diagonalization matrix *DIAG* is obtained using Eq.(39) with Eqs. (36) and (51) so that (Mathematica, 1991)

$$
\begin{aligned}
DIAG &= DIA^T QM\ DIA \\
&= \begin{bmatrix}
q_{11} + q_{12}s_0 + q_{21}s_0 + q_{13}t_0 + q_{31}t_0 & q_{12}\cos\theta + q_{13}\sin\theta & q_{13}\cos\theta - q_{12}\sin\theta \\
q_{12}\cos\theta + q_{13}\sin\theta & 0 & 0 \\
q_{13}\cos\theta - q_{12}\sin\theta & 0 & 0
\end{bmatrix}
\end{aligned} \tag{53}
$$

or, noting the symmetry in Eq.(53),

$$
DIAG = \begin{bmatrix}
d_{11} & d_{12} & d_{13} \\
d_{12} & d_{22} & d_{23} \\
d_{13} & d_{23} & d_{33}
\end{bmatrix}, \tag{54}
$$

where

$$
\begin{aligned}
d_{11} &= q_{11} + q_{12}s_0 + q_{21}s_0 + q_{13}t_0 + q_{31}t_0 \\
d_{12} &= q_{12}\cos\theta + q_{13}\sin\theta \\
d_{13} &= q_{13}\cos\theta - q_{12}\sin\theta\,,
\end{aligned} \tag{55}
$$

and

$$
d_{22}^D = d_{23}^D = d_{33}^D = 0\,. \tag{56}
$$

Next, if Eq.(53) is to be a diagonal matrix, then the off-diagonal elements must be zero. From Eq.(53)–(55), this means that we have the conditions

$$
d_{12}^D = d_{13}^D = 0\,, \tag{57}
$$

so that

$$\cos\theta = \frac{q_{12}}{q_{13}}\sin\theta$$
$$\cos\theta = -\frac{q_{13}}{q_{12}}\sin\theta\,, \tag{58}$$

which we shall make use of momentarily.

When the surface intersecting the plot plane is a plane, the conditions in Eq.(56) cause Eq.(42) to reduce to

$$I^D = d_{11}^D + d_{12}^D u + d_{13}^D v = 0\,, \tag{59}$$

which is the equation of a line. Using the expressions in Eq.(55),

$$I^D = q_{11} + 2q_{12}s_0 + 2q_{13}t_0 + 2\left(q_{12}\cos\theta + q_{13}\sin\theta\right)u + 2\left(q_{13}\cos\theta - q_{12}\sin\theta\right)v = 0\,. \tag{60}$$

Now, insert the diagonalization conditions given in Eqs.(58) to obtain the two expressions

$$\frac{q_{11}q_{12}}{2\left(q_{12}^2+q_{13}^2\right)} + \frac{q_{12}^2 s_0}{q_{12}^2+q_{13}^2} + \frac{q_{12}q_{13}t_0}{q_{12}^2+q_{13}^2} - v\sin\theta = 0$$
$$\frac{q_{11}q_{13}}{2\left(q_{12}^2+q_{13}^2\right)} + \frac{q_{12}q_{13}s_0}{q_{12}^2+q_{13}^2} + \frac{q_{13}^2 t_0}{q_{12}^2+q_{13}^2} + u\sin\theta = 0\quad. \tag{61}$$

Solving the expressions in Eq.(61) for u and v, we get

$$v = \frac{1}{\sin\theta}\left[\frac{q_{11}q_{12}}{2\left(q_{12}^2+q_{13}^2\right)} + \frac{q_{12}^2 s_0}{q_{12}^2+q_{13}^2} + \frac{q_{12}q_{13}t_0}{q_{12}^2+q_{13}^2}\right]$$
$$u = -\frac{1}{\sin\theta}\left[\frac{q_{11}q_{13}}{2\left(q_{12}^2+q_{13}^2\right)} + \frac{q_{12}q_{13}s_0}{q_{12}^2+q_{13}^2} + \frac{q_{13}^2 t_0}{q_{12}^2+q_{13}^2}\right]\quad. \tag{62}$$

Let us now make use of Eqs.(35) and (36) to write

$$
\begin{aligned}
s &= s_0 + \cos\theta\, u - \sin\theta\, v \\
t &= t_0 + \sin\theta\, u - \cos\theta\, v \quad .
\end{aligned}
\tag{63}
$$

Substituting the expressions for u and v from Eq.(62) into Eq.(63) give s and t as

$$
\begin{aligned}
s = s_0 &+ \cos\theta\left\{-\frac{1}{\sin\theta}\left[\frac{q_{11}q_{13}}{2\left(q_{12}^2+q_{13}^2\right)}+\frac{q_{12}q_{13}s_0}{q_{12}^2+q_{13}^2}+\frac{q_{13}^2t_0}{q_{12}^2+q_{13}^2}\right]\right\} \\
&- \sin\theta\left\{\frac{1}{\sin\theta}\left[\frac{q_{11}q_{12}}{2\left(q_{12}^2+q_{13}^2\right)}+\frac{q_{12}^2s_0}{q_{12}^2+q_{13}^2}+\frac{q_{12}q_{13}t_0}{q_{12}^2+q_{13}^2}\right]\right\} \\
t = t_0 &+ \sin\theta\left\{-\frac{1}{\sin\theta}\left[\frac{q_{11}q_{13}}{2\left(q_{12}^2+q_{13}^2\right)}+\frac{q_{12}q_{13}s_0}{q_{12}^2+q_{13}^2}+\frac{q_{13}^2t_0}{q_{12}^2+q_{13}^2}\right]\right\} \\
&+ \cos\theta\left\{\frac{1}{\sin\theta}\left[\frac{q_{11}q_{12}}{2\left(q_{12}^2+q_{13}^2\right)}+\frac{q_{12}^2s_0}{q_{12}^2+q_{13}^2}+\frac{q_{12}q_{13}t_0}{q_{12}^2+q_{13}^2}\right]\right\} \quad .
\end{aligned}
\tag{64}
$$

Rewriting Eq.(64) as

$$
\begin{aligned}
s &= -\frac{q_{11}q_{12}}{2\left(q_{12}^2+q_{13}^2\right)}-\frac{q_{12}^2s_0}{q_{12}^2+q_{13}^2}-\frac{q_{12}q_{13}t_0}{q_{12}^2+q_{13}^2}+s_0-\frac{\cos\theta}{\sin\theta}\left[\frac{q_{11}q_{13}}{2\left(q_{12}^2+q_{13}^2\right)}+\frac{q_{12}q_{13}s_0}{q_{12}^2+q_{13}^2}+\frac{q_{13}^2t_0}{q_{12}^2+q_{13}^2}\right] \\
t &= -\frac{q_{11}q_{13}}{2\left(q_{12}^2+q_{13}^2\right)}-\frac{q_{12}q_{13}s_0}{q_{12}^2+q_{13}^2}-\frac{q_{13}^2t_0}{q_{12}^2+q_{13}^2}+t_0+\frac{\cos\theta}{\sin\theta}\left[\frac{q_{11}q_{12}}{2\left(q_{12}^2+q_{13}^2\right)}+\frac{q_{12}^2s_0}{q_{12}^2+q_{13}^2}+\frac{q_{12}q_{13}t_0}{q_{12}^2+q_{13}^2}\right]
\end{aligned}
\tag{65}
$$

facilitates factoring to give

$$
\begin{aligned}
s &= -\frac{q_{11}q_{12}}{2\left(q_{12}^2+q_{13}^2\right)} \\
&\quad +\frac{s_0}{q_{12}^2+q_{13}^2}\left[q_{13}^2-\frac{\cos\theta}{\sin\theta}q_{12}q_{13}\right]-\frac{t_0}{q_{12}^2+q_{13}^2}\left[q_{11}q_{13}+\frac{\cos\theta}{\sin\theta}q_{13}^2\right]-\frac{\cos\theta}{\sin\theta}\frac{q_{11}q_{13}}{2\left(q_{12}^2+q_{13}^2\right)} \\
t &= -\frac{q_{11}q_{13}}{2\left(q_{12}^2+q_{13}^2\right)} \\
&\quad +\frac{s_0}{q_{12}^2+q_{13}^2}\left[\frac{\cos\theta}{\sin\theta}q_{12}^2-q_{12}q_{13}\right]+\frac{t_0}{q_{12}^2+q_{13}^2}\left[q_{12}^2+\frac{\cos\theta}{\sin\theta}q_{12}q_{13}\right]+\frac{\cos\theta}{\sin\theta}\frac{q_{11}q_{12}}{2\left(q_{12}^2+q_{13}^2\right)}
\end{aligned}
\tag{66}
$$

which simplifies to

$$\begin{aligned} s &= -\frac{q_{11}q_{12}}{2\left(q_{12}^2+q_{13}^2\right)}+q_{13}p \\ t &= -\frac{q_{11}q_{13}}{2\left(q_{12}^2+q_{13}^2\right)}-q_{12}p\,, \end{aligned} \tag{67}$$

where

$$p=\frac{s_0}{q_{12}^2+q_{13}^2}\left[q_{13}-\frac{\cos\theta}{\sin\theta}q_{12}\right]-\frac{t_0}{q_{12}^2+q_{13}^2}\left[q_{11}+\frac{\cos\theta}{\sin\theta}q_{13}\right]-\frac{\cos\theta}{\sin\theta}\frac{q_{11}}{2\left(q_{12}^2+q_{13}^2\right)}. \tag{68}$$

Clearly $-\infty \le p \le \infty$. Eq.(67) can be written as the following parametric curves for a plane intersecting a plot plane, i.e., the parametric equations of a 2-D line,

$$\begin{aligned} s &= C_1 + C_2 p \\ t &= C_4 + C_5 p \end{aligned} \tag{69}$$

where the expressions for C_1, C_2, C_4, and C_5 are

$$C_1=\frac{-0.5q_{11}q_{12}}{q_{12}^2+q_{13}^2}, C_2=q_{13}, C_4=\frac{-0.5q_{11}q_{13}}{q_{12}^2+q_{13}^2}, C_5=-q_{12}. \tag{70}$$

Equations(69) and (70) constitute the expressions that are used to plot the intersection of a plane with the MCNP plot plane using a general quadratic expression for the conic as given by Eq.(25). Values of p are selected and used with C_1, C_2, C_4, and C_5 to calculate values of s and t. The C_1, C_2, C_4, and C_5 contain the *QM* coefficients, which from Eq.(49) are composed of the plot-command coefficients and the coefficients of the 3-D surface intersecting the plot plane. Equation(69) is listed in the MCNP theory manuals beginning in 1979 (Thompson, 1979) without the values C_1, C_2, C_4, and C_5 given in Eq.(70). Inspection of MCNPX coding reveals that Eq.(69) is contained in subroutine **ptost.F** as pg.13–pg.14, while Eq.(70) is contained subroutine **regula.F** as rg.37-rg.50.

4.2. Intersection of a sphere with the plot plane

As another illustration of the procedure that is used to develop a one-parameter expression for a 3-D surface in the plot plane, let us examine the case when the 3-D surface is a sphere. For a sphere, Eq.(20) simplifies to

$$A^G(x^G)^2 + B^G(y^G)^2 + C^G(z^G)^2 + G^G x^G + H^G y^G + J^G z^G + K^G = 0 \quad , \tag{71}$$

which has the matrix representation given by Eq. (5),

$$\begin{bmatrix} 1 & x^G & y^G & x^G \end{bmatrix} AM^G \begin{bmatrix} 1 \\ x^G \\ y^G \\ z^G \end{bmatrix} = 0 \, , \tag{72}$$

with the coefficient matrix given by Eq. (3) written as

$$AM^G = \begin{bmatrix} K^G & G^G/2 & H^G/2 & J^G/2 \\ G^G/2 & A^G & 0 & 0 \\ H^G/2 & 0 & B^G & 0 \\ J^G/2 & 0 & 0 & C^G \end{bmatrix} . \tag{73}$$

The expression for a sphere in plot-plane coordinates is given by Eq.(31) which, owing to the symmetry of the matrix AM^G in Eq.(73), is (Mathematica, 1991)

$$QM = \begin{bmatrix} q_{11} & q_{12} & q_{13} \\ q_{12} & q_{22} & q_{23} \\ q_{13} & q_{23} & q_{33} \end{bmatrix} = \begin{bmatrix} C^P & G^P & F^P \\ G^P & A^P & H^P \\ F^P & H^P & B^P \end{bmatrix} , \tag{74}$$

with the matrix coefficients

$$
\begin{aligned}
q_{11} &= A^G x_0^2 + B^G y_0^2 + C^G z_0^2 + G^G x_0 + H^G y_0 + J^G z_0 + K^G \\
q_{12} &= A^G a_x x_0 + B^G a_y y_0 + C^G a_z z_0 + \frac{1}{2}\left(a_x G^G + a_y H^G + a_z J^G\right) \\
q_{13} &= A^G b_x x_0 + B^G b_y y_0 + C^G b_z z_0 + \frac{1}{2}\left(b_x G^G + b_y H^G + b_z J^G\right) \\
q_{22} &= A^G a_x^2 + B^G a_y^2 + C^G a_z^2 \\
q_{23} &= A^G a_x b_x + B^G a_y b_y + C^G a_z b_z \\
q_{33} &= A^G b_x^2 + B^G b_y^2 + C^G b_z^2 \ .
\end{aligned}
\tag{75}
$$

Next, a formulation and solution to Eq.(41) for the case of a sphere intersecting the plot plane is developed. First, the diagonalization matrix *DIAG* is obtained using Eq.(39) with Eqs. (36) and (74) to obtain

$$
DIAG = \begin{bmatrix} d_{11} & d_{12} & d_{13} \\ d_{12} & d_{22} & d_{23} \\ d_{13} & d_{23} & d_{33} \end{bmatrix},
\tag{76}
$$

where

$$
\begin{aligned}
d_{11} &= q_{11} + 2q_{12}s_0 + q_{22}s_0^2 + 2q_{13}t_0 + 2q_{23}s_0t_0 + q_{33}t_0^2 \\
d_{12} &= \cos\theta\left(q_{12} + q_{22}s_0 + q_{23}t_0\right) + \sin\theta\left(q_{13} + q_{23}s_0 + q_{33}t_0\right) \\
d_{13} &= -\sin\theta\left(q_{12} + q_{22}s_0 + q_{23}t_0\right) + \cos\theta\left(q_{13} + q_{23}s_0 + q_{33}t_0\right) \\
d_{22} &= \cos\theta\left(q_{22}\cos\theta + q_{23}\sin\theta\right) + \sin\theta\left(q_{23}\cos\theta + q_{33}\sin\theta\right) \\
d_{23} &= \cos\theta\left(q_{23}\cos\theta - q_{22}\sin\theta\right) + \sin\theta\left(q_{33}\cos\theta - q_{23}\sin\theta\right) \\
d_{33} &= -\sin\theta\left(q_{23}\cos\theta - q_{22}\sin\theta\right) + \cos\theta\left(q_{33}\cos\theta - q_{23}\sin\theta\right) \quad .
\end{aligned}
\tag{77}
$$

Next, if Eq.(76) is to be a diagonal matrix, then the off-diagonal elements must be zero. Thus,

$$
d_{12}^D = d_{13}^D = d_{23}^D = 0 \, .
\tag{78}
$$

The conditions in Eq.(78) will be used shortly.

For the case of the intersection of a sphere with the plot plane, Eq. (41), i.e.,

$$I = \begin{bmatrix} 1 & u & v \end{bmatrix} DIA^T QM\ DIA \begin{bmatrix} 1 \\ u \\ v \end{bmatrix} = 0 \tag{79}$$

is

$$I = d_{11} + 2d_{12}u + 2d_{13}v + 2d_{23}uv + d_{22}u^2 + d_{33}v^2 = 0\,. \tag{80}$$

For the sake of an explicit expression, use of the expressions in Eq.(77) in Eq. (80) gives

$$\begin{aligned} I = {} & q_{11} + 2q_{12}s_0 + q_{22}s_0^2 + 2q_{13}t_0 + 2q_{23}s_0t_0 + q_{33}t_0^2 \\ & +2\left[\cos\theta\left(q_{12} + q_{22}s_0 + q_{23}t_0\right) + \sin\theta\left(q_{13} + q_{23}s_0 + q_{33}t_0\right)\right]u \\ & +2\left[-\sin\theta\left(q_{12} + q_{22}s_0 + q_{23}t_0\right) + \cos\theta\left(q_{13} + q_{23}s_0 + q_{33}t_0\right)\right]v \\ & +2\left[\cos\theta\left(q_{23}\cos\theta - q_{22}\sin\theta\right) + \sin\theta\left(q_{33}\cos\theta - q_{23}\sin\theta\right)\right]uv \\ & +\left[\cos\theta\left(q_{22}\cos\theta + q_{23}\sin\theta\right) + \sin\theta\left(q_{23}\cos\theta + q_{33}\sin\theta\right)\right]u^2 \\ & +\left[-\sin\theta\left(q_{23}\cos\theta - q_{22}\sin\theta\right) + \cos\theta\left(q_{33}\cos\theta - q_{23}\sin\theta\right)\right]v^2 \quad . \end{aligned} \tag{81}$$

This expression contains linear and quadratic terms in u and v. This will necessitate modifications to the solution process followed for the case of a plane intersecting a plot plane, where, Eq.(59), only linear terms in *u* and *v* existed.

To proceed, the diagonalization conditions in Eq.(78) are used. These conditions with the expressions in Eq.(77) constitute three equations in the three unknown variables s_0, t_0 and θ. The expression for d_{23} contains only the angle θ, so we can solve $d_{23}^D = 0$ for the angle θ^D as given in Eq.(45).

Next, we substitute the angle θ^D from Eq.(45) into the expressions for d_{12} and d_{13} in Eq.(77) to obtain two coupled equations involving the two unknowns s_0 and t_0. Solving these equations gives (after some algebra)

$$s_0 = \frac{q_{13}q_{23} - q_{12}q_{33}}{q_{22}q_{33} - q_{23}^2} \tag{82}$$

$$t_0 = \frac{q_{12}q_{23} - q_{13}q_{22}}{q_{22}q_{33} - q_{23}^2} \tag{83}$$

as the values for the translation involved in the diagonalization process. These values are coded in subroutine **regula.F** as rg.77 and rg.78.

With the diagonalization conditions of Eq.(78) and the diagonalization parameters in Eqs.(45), (82), and (83), the equation of the conic for a sphere intersecting the plot plane given by Eq.(80) reduces to

$$I^D = d_{11}^D + d_{22}^D u^2 + d_{33}^D v^2 = 0\,, \tag{84}$$

where d_{11}^D, d_{22}^D, and d_{33}^D are d_{11}, d_{22}, and d_{33} given in Eq.(77) evaluated using the diagonalization parameters θ^D, s_0, and t_0 given in Eqs. (45), (82), and (83). The diagonalization process means that Eq.(84) can be written using a one-parameter set of relationships of the form $u = u(p)$ and $v = v(p)$. So expressions for $u = u(p)$ and $v = v(p)$ are sought which satisfy Eq.(84).

In general, the form of $u = u(p)$ and $v = v(p)$ is dependent upon the signs of d_{11}^D, d_{22}^D, and d_{33}^D. It can be shown from analytic geometry (Tierney, pp. 226–230) that the following conics exist:

$$
\begin{aligned}
&d_{22}^D d_{33}^D > 0 : \text{ellipse, circle, point, or imaginary} \\
&d_{22}^D d_{33}^D < 0 : \text{hyperbola, or, two, intersecting lines} \\
&d_{22}^D d_{33}^D = 0 : \text{parabola, a, line, or two parallel lines or imaginary} \quad ,
\end{aligned}
\tag{85}
$$

where the case $d_{22}^D d_{33}^D = 0$ has either $d_{22}^D \neq 0$ or $d_{33}^D \neq 0$.

The intersection of a sphere with a plane is an ellipse, circle, or a point. Consequently, $d_{22}^D d_{33}^D > 0$. Thus, the selection

$$
\begin{aligned}
u(p) &= \sqrt{-\frac{d_{11}^D}{d_{22}^D}} \cos p \\
v(p) &= \sqrt{-\frac{d_{11}^D}{d_{33}^D}} \sin p
\end{aligned}
\tag{86}
$$

causes Eq.(84) to be satisfied. The square-root quantities in Eq.(86) are coded in **regula.F** as rg.111 and rg.112, while the trigonometric quantites are coded in **regula.F** as rg.68 and rg.70.

Using the formulas in Eq.(86), a univariate set of expressions $s = s(p)$ and $t = t(p)$ are obtained for a sphere intersecting the plot plane. From Eq.(34),

$$
\begin{aligned}
s &= s_0 + \cos\theta\, u - \sin\theta\, v \\
t &= t_0 + \sin\theta\, u - \cos\theta\, v \quad .
\end{aligned}
\tag{87}
$$

Using the diagonalization values θ^D, s_0, and t_0 given in Eqs. (45), (82), and (83) and inserting Eq.(86) gives

$$
\begin{aligned}
s &= C_1 + C_2 \sin p + C_3 \cos p \\
t &= C_4 + C_5 \sin p + C_6 \cos p \, ,
\end{aligned}
\tag{88}
$$

where the expressions for $C_1 - C_6$ are

$$C_1 = s_0, \quad C_2 = -\sin\theta^D \sqrt{-\frac{d_{11}^D}{d_{33}^D}}, \quad C_3 = \cos\theta^D \sqrt{-\frac{d_{11}^D}{d_{22}^D}}$$
$$C_4 = t_0, \quad C_5 = -\cos\theta^D \sqrt{-\frac{d_{11}^D}{d_{33}^D}}, \quad C_6 = \sin\theta^D \sqrt{-\frac{d_{11}^D}{d_{22}^D}}, \tag{89}$$

which are coded in **ptost.F** as pj.25 and pg.26.

4.3. Intersection of other surfaces with the plot plane

The analysis in Section 4.2 is valid for surfaces, including a sphere, whose intersection with the plot plane is an ellipse. We next consider the cases when the intersection of a 3-D surface with the plot plane causes a hyperbola or a parabola to be formed.

Consider the case of a hyperbola. The intersection of a 3-D surface with the plot plane given by Eq.(41),

$$I = \begin{bmatrix} 1 & u & v \end{bmatrix} DIA^T QM\ DIA \begin{bmatrix} 1 \\ u \\ v \end{bmatrix} = 0, \tag{90}$$

or as written in the form of Eq.(42),

$$I = d_{11} + 2d_{12}u + 2d_{13}v + 2d_{23}uv + d_{22}u^2 + d_{33}v^2 = 0. \tag{91}$$

Applying diagonalization so that the off-diagonal elements are set to zero,

$$d_{12}^D = d_{13}^D = d_{23}^D = 0, \tag{92}$$

the bivariate quadratic reduces to a form with only quadratic terms

$$I^D = d_{11}^D + d_{22}^D u^2 + d_{33}^D v^2 = 0. \tag{93}$$

According to the conditions in Eq.(85), for a hyperbola the signs of d_{22}^D and d_{33}^D differ. In this situation, recalling that

$$\cosh^2 x - \sinh^2 x = 1, \tag{94}$$

the selection

$$\begin{aligned} u(p) &= \sqrt{\frac{d_{11}^D}{d_{22}^D}} \sinh p \\ v(p) &= \sqrt{-\frac{d_{11}^D}{d_{33}^D}} \cosh p \end{aligned} \tag{95}$$

causes Eq.(84) to be satisfied. Inserting the expressions in Eq.(95) into Eq.(34) gives

$$\begin{aligned} s &= C_1 + C_2 \sinh p + C_3 \cosh p \\ t &= C_4 + C_5 \sinh p + C_6 \cosh p\,, \end{aligned} \tag{96}$$

where the expressions for $C_1 - C_6$ are

$$\begin{aligned} &C_1 = s_0, \quad C_2 = \cos\theta^D \sqrt{\frac{d_{11}^D}{d_{22}^D}}, \quad C_3 = -\sin\theta^D \sqrt{-\frac{d_{11}^D}{d_{33}^D}} \\ &C_4 = t_0, \quad C_5 = \sin\theta^D \sqrt{\frac{d_{11}^D}{d_{22}^D}}, \quad C_6 = -\cos\theta^D \sqrt{-\frac{d_{11}^D}{d_{33}^D}}\,, \end{aligned} \tag{97}$$

as the one-parameter set of expressions $s = s(p)$ and $t = t(p)$ for any surface intersecting the plot plane which results in a hyperbolic conic. The formulas in Eq.(97) are coded in regula.F lines rg.127–rg.135 and rg.144–rg.145, while the expressions in Eq.(96) are coded in **ptost.F** as pj.32 and pg.33.

For the case of a parabola we return to Eq.(42),

$$I = d_{11} + 2d_{12}u + 2d_{13}v + 2d_{23}uv + d_{22}u^2 + d_{33}v^2 = 0 \tag{98}$$

The axis-rotation, or, equivalently, the congruency transformation, eliminates the *uv* term to give the bivariate quadratic

$$I^D = d_{11}^D + 2d_{12}^D u + 2d_{13}^D v + d_{22}^D u^2 + d_{33}^D v^2 = 0\,. \tag{99}$$

From analytic geometry, Eq.(99) is a general parabola when either $d_{22}^D = 0$ or $d_{33}^D = 0$. In addition, when $d_{22}^D = 0$ we can take $d_{13}^D = 0$ to have a parabola whose vertex is the *u*-axis. For the case $d_{22}^D = 0$ and $d_{13}^D = 0$ (MCNPX **regula.F** index J=3), the congruency transformation matrix is

$$DIAG = \begin{bmatrix} d_{11}^D & d_{12}^D & 0 \\ d_{12}^D & 0 & 0 \\ 0 & 0 & d_{33}^D \end{bmatrix}. \tag{100}$$

Eq.(99) reduces to

$$I^D = d_{11}^D + 2d_{12}^D u + d_{33}^D v^2 = 0\,, \tag{101}$$

which is satisfied by selecting

$$\begin{aligned} u(p) &= -\frac{1}{2}\left(\frac{d_{33}^D}{d_{12}^D} p^2 + \frac{d_{11}^D}{d_{12}^D} \right) \\ v(p) &= p\,. \end{aligned} \tag{102}$$

Inserting the expressions in Eq.(102) into Eq.(34) gives

$$\begin{aligned} s &= C_1 + C_2 p + C_3 p^2 \\ t &= C_4 + C_5 p + C_6 p^2\,, \end{aligned} \tag{103}$$

where $C_1 - C_6$ are

$$\begin{aligned} C_1 &= s_0 - \frac{1}{2}\frac{d_{11}^D}{d_{12}^D}\cos\theta^D, \quad C_2 = -\sin\theta^D, \quad C_3 = \frac{1}{2}\frac{d_{33}^D}{d_{12}^D}\cos\theta^D \\ C_4 &= t_0 - \frac{1}{2}\frac{d_{11}^D}{d_{12}^D}\sin\theta^D, \quad C_5 = \cos\theta^D, \quad C_6 = -\frac{1}{2}\frac{d_{33}^D}{d_{12}^D}\sin\theta^D\,. \end{aligned} \tag{104}$$

For the case $d_{33}^D = 0$ (MCNPX **regula.F** index J=2), we can take $d_{12}^D = 0$ to obtain a parabola whose vertex is the *v*-axis. For the case $d_{22}^D = 0$ and $d_{12}^D = 0$ (J=3), the congruency transformation matrix is

$$DIAG = \begin{bmatrix} d_{11}^D & 0 & d_{13}^D \\ 0 & d_{22}^D & 0 \\ d_{13}^D & 0 & 0 \end{bmatrix}. \tag{105}$$

Eq.(99) reduces to

$$I^D = d_{11}^D + 2d_{13}^D v + d_{22}^D u^2 = 0\,, \tag{106}$$

which is satisfied by the selections

$$\begin{aligned} u(p) &= p \\ v(p) &= -\frac{1}{2}\left(\frac{d_{22}^D}{d_{13}^D} p^2 + \frac{d_{11}^D}{d_{13}^D} \right). \end{aligned} \tag{107}$$

Inserting the formulas in Eq.(107) into Eq.(34) gives

$$\begin{aligned} s &= C_1 + C_2 p + C_3 p^2 \\ t &= C_4 + C_5 p + C_6 p^2\,, \end{aligned} \tag{108}$$

where the expressions for $C_1 - C_6$ are

$$\begin{aligned} C_1 &= s_0 + \frac{1}{2}\frac{d_{11}^D}{d_{13}^D}\sin\theta^D, \quad C_2 = \cos\theta^D, \quad C_3 = \frac{1}{2}\frac{d_{22}^D}{d_{13}^D}\sin\theta^D \\ C_4 &= t_0 + \frac{1}{2}\frac{d_{11}^D}{d_{13}^D}\cos\theta^D, \quad C_5 = \sin\theta^D, \quad C_6 = -\frac{1}{2}\frac{d_{22}^D}{d_{13}^D}\cos\theta^D\,. \end{aligned} \tag{109}$$

The constants in Eqs.(104) and (109) are coded in **regula.F** lines rg.99–rg.104 and rg.144–rg.145, while Eq.(108) is evaluated in **ptost.F** pj.18–pj.19.

5. Geometry plotter: intersection of two curves in the plot plane

Functionality of the geometry plotter includes the determination of the POIs of curves in the plot plane. The curves are created by the intersections of the 3-D surfaces with the plot plane. The POIs are determined in plot-space (s, p) coordinates. These points are used to determine the identity of cells on either side of the curve connecting the POIs and the type of curve connecting the POIs. For graphic visualization a solid line is used to distinguish differing cells on either side of the curve, no line is used when identical cells lie on either side of the curve, and a dashed line is used to highlight instances involving geometry problems or ambiguities.

These concepts are illustrated in the following plots that were created using the MCNP interactive geometry plotter. The model consists of a sphere containing two boxes. The relevant geometry is listed in Appendix 1. Each plot shows the image in the plot plane at z = 0 with extent 5 and with cell and surface labeling activated.

Figure 4 shows the plotted geometry for the correct model. The cell numbers are labeled in red; the sphere is cell 1 and the boxes cells 2 and 3. The surface numbers are labeled in black; the sphere is defined by surface 1, cell 2 by surfaces 10–13, and cell 3 by surfaces 20–23. For this model the geometry is well defined and all surfaces are plotted using solid black lines.

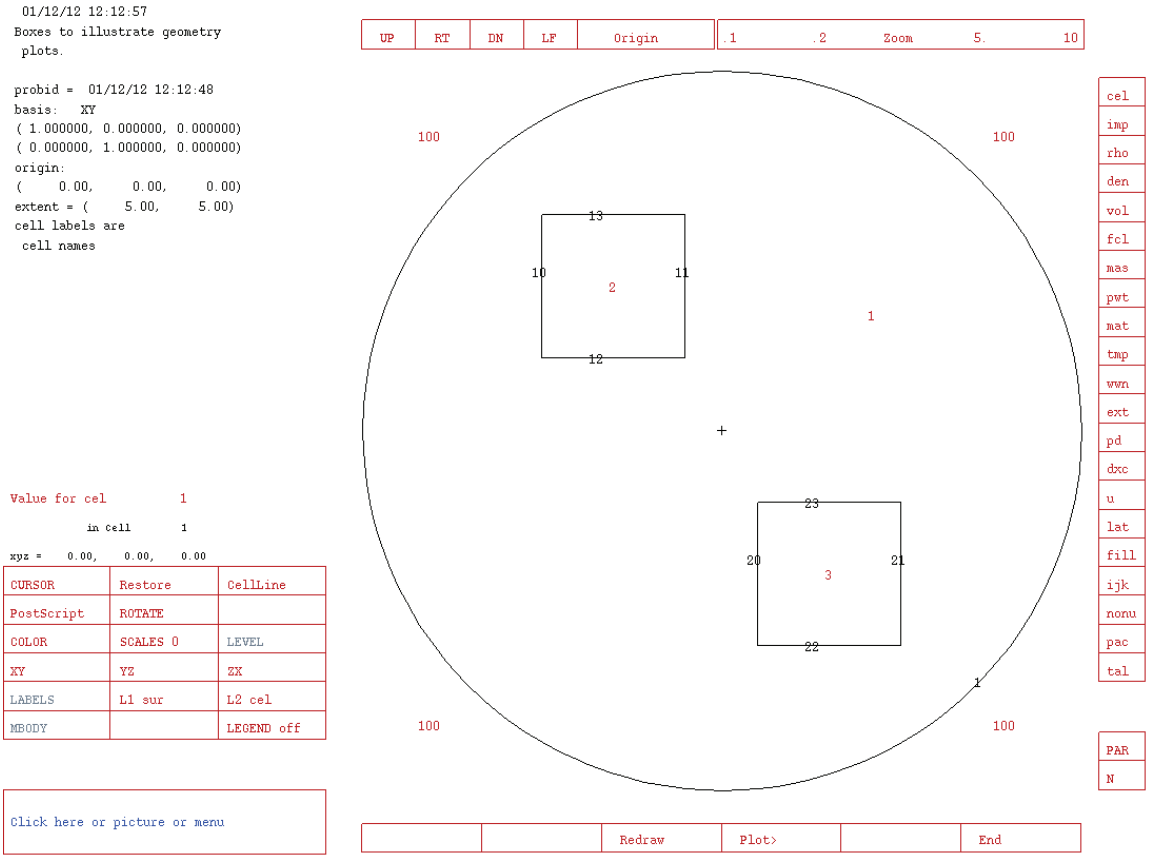

Figure 4. Geometry plot for the correct model.

Figure 5 shows the plotted geometry for a faulty model. The error in this model was created by omitting "#3" in the description of cell 1. The symbol # is the complement operator which is used to designate *not in*.[†] Thus, cell 3 is specified, but cell 1 lacks the information necessary to recognize its presence. Consequently, the surfaces for cell 3 are plotted using dotted red lines. The plot legend signals the geometry error. The presence of cell 1 inside of the sphere is unaffected, so it is plotted using solid black lines.

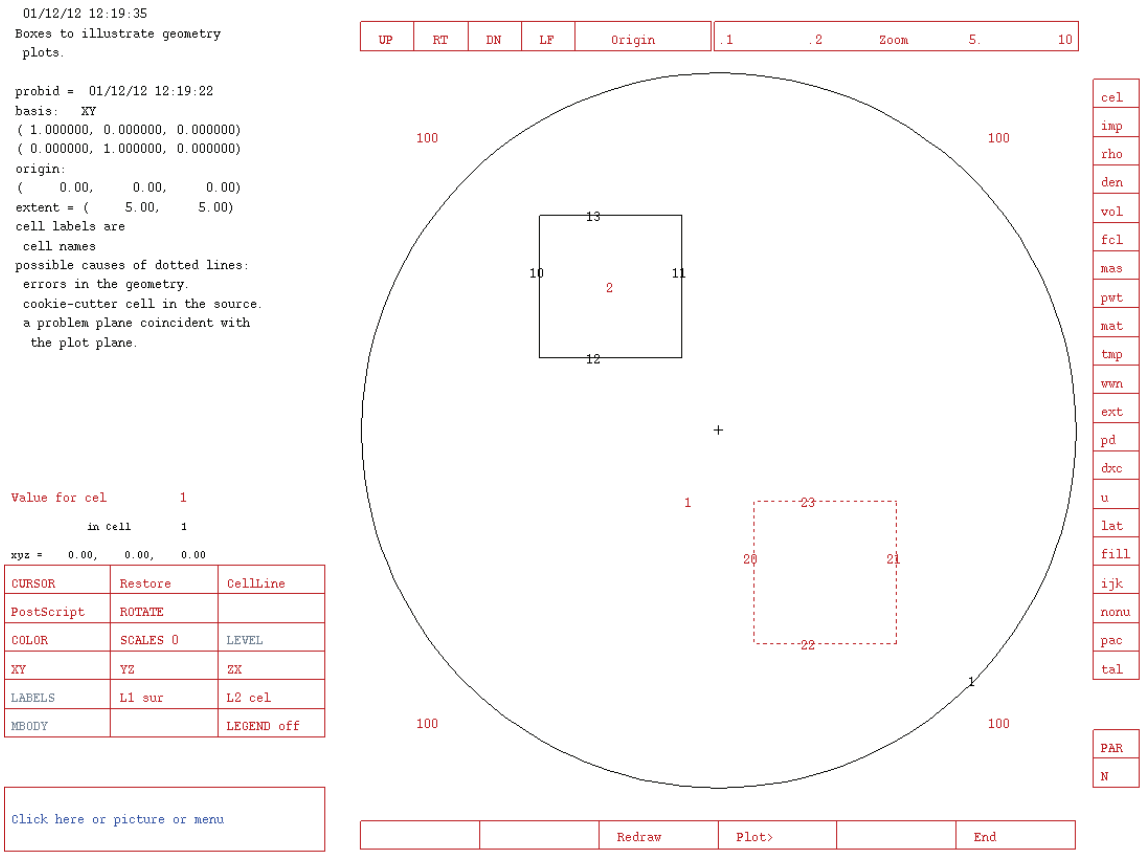

Figure 5. Geometry plot for error created by omitting #3 in the description of cell 1.

[†] The complement operator is just a shorthand cell-specification method that implicitly uses the intersection and union operator. Details describing the combinatorial geometry feature in MCNP are provided in the manual (Pelowitz, 2011).

Figure 6 contains the plotted geometry for a model in which surface 23 of cell 3 erroneously has been assigned a positive rather than a negative sense; i.e., +23 instead of –23. This error causes the description of cell 3 to be incorrect which causes the configuration of cell 3 to be incorrect. The three sides of cell 3 are plotted using solid black lines. The upper boundary of cell 3 intersects the sphere and is plotted using a dotted red line. The plot legend signals the geometry error. As with the previous model, cell 1 is correctly specified and is plotted using solid black lines.

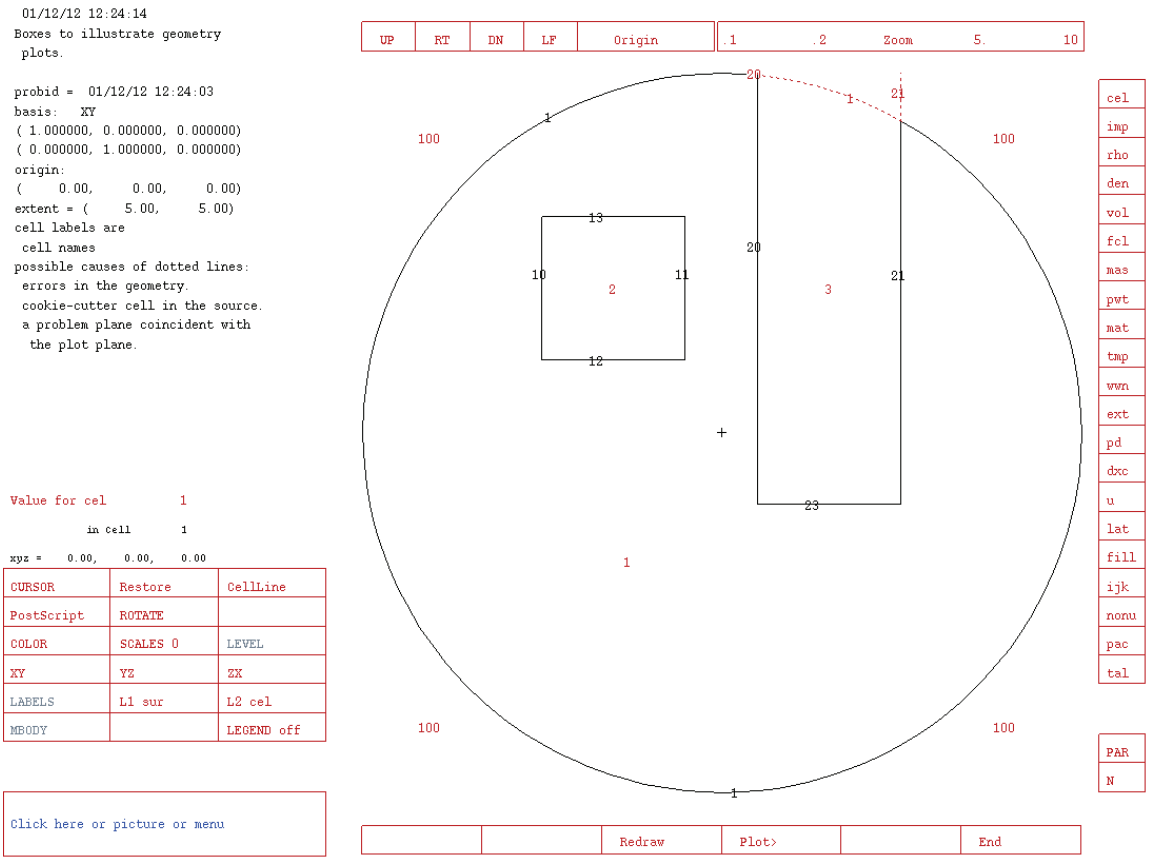

Figure 6. Geometry plot for error created by incorrectly specifying surface 23 of cell 3 with a positive sense.

The model used to plot Fig. 7 contains two errors: a positive sense for surface 23 of cell 3 and for surface 11 of cell 2. These errors cause the distortion of both boxes, cells 2 and 3. Without delving into the combinatorial geometry, suffice it to say that cells 2 and 3 erroneously overlap each other which results in boundaries that are plotted using solid black lines and dotted red lines. The boundaries of cells 2 and 3 intersected with the sphere and those sections are plotted as dotted red lines. The plot legend signals the geometry error.

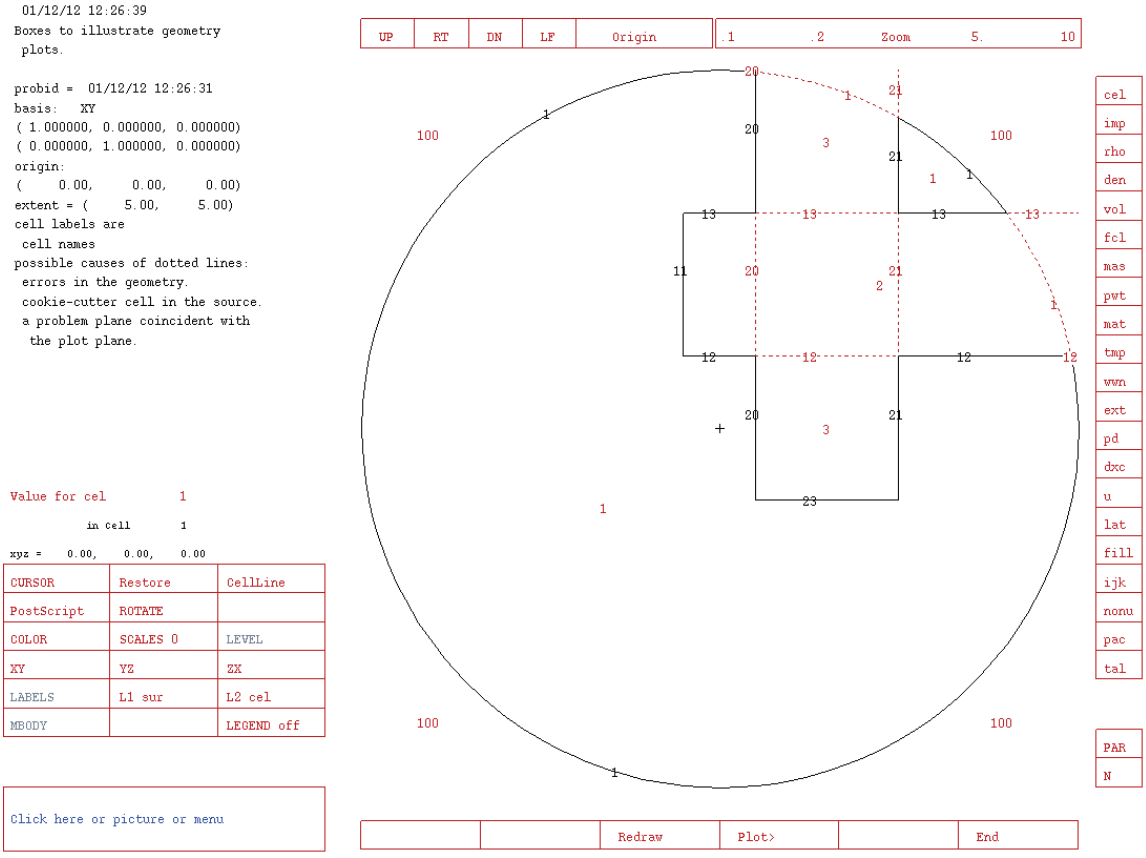

Figure 7. Geometry plot displaying errors created by incorrectly specifying surface 23 of cell 3 and surface 11 of cell 2 as having a positive sense.

For each of the models plotted in Figs. 4–7, MCNP uses a combination of Boolean logic[†] and analytic geometry algorithms to determine and plot the geometry. These algorithms create a geometry recognition capability that makes the geometry plotter a powerful debugging tool for MCNP users. We do not delve into the Boolean logic aspect of the geometry plotter in this article. However, next we do present some of the analytic-geometry formulations that are used to determine the POI for curves in the plot plane. These formulations have not been previously documented.

5.1. Intersection of two lines in the plot plane

The POI of two lines in the plot plane is derived using the parametric form of a line as given by Eq.(69). For line 1

$$\begin{aligned} s &= C_1 + C_2 p \\ t &= C_4 + C_5 p \end{aligned} \tag{110}$$

and line 2

$$\begin{aligned} s &= D_1 + D_2 q \\ t &= D_4 + D_5 q \end{aligned} . \tag{111}$$

These are lines through the points $P_0(C_1, C_4)$ and $Q_0(D_1, D_4)$ in the directions $\vec{A} = C_2\hat{i} + C_5\hat{j}$ and $\vec{B} = D_2\hat{i} + D_5\hat{j}$ (Tierney, p. 438).

The POI is derived by equating *s* and *t* in Eqs.(110) and (111) so that

$$\begin{aligned} C_1 + C_2 p &= D_1 + D_2 q \\ C_4 + C_5 p &= D_4 + D_5 q \end{aligned} . \tag{112}$$

Solving the second expression in Eq.(112) for *q* gives

[†] Boolean logic is also used for particle tracking.

$$q = \frac{C_4 + C_5 p - D_4}{D_5}. \tag{113}$$

Substituting this result into the first expression in Eq.(112) and solving for p gives

$$p = \frac{D_5\left(D_1 - C_5\right) + D_2\left(C_4 - D_4\right)}{C_2 D_5 - D_2 C_5}. \tag{114}$$

The result in Eq.(114) is coded as "*a*" in **inter.F** line in.87 and is stored in the array crs(nxp) as the location of the intersection of two lines.

Two vectors are parallel if their cross product is zero. Thus, here we calculate

$$\hat{A} \times \hat{B} = C_2 D_5 - D_2 C_5, \tag{115}$$

which is the denominator of Eq.(114) and is coded as "*b*" in **inter.F** line in.85, can be used as a check to assess whether the two lines intersect.

5.2. Intersection of a line and a quadratic in the plot plane

The POI of a line and a quadratic in the plot plane is derived using the parametric form of a line as given by Eq.(69) and the equation of a general quadratic as given by Eq.(32). For the line

$$\begin{aligned} s &= C_1 + C_2 p \\ t &= C_4 + C_5 p \end{aligned} \tag{116}$$

and the quadratic

$$q_{22} s^2 + 2q_{23} st + q_{33} t^2 + 2q_{12} s + 2q_{13} t + q_{11} = 0. \tag{117}$$

Substitution of the expressions for *s* and *t* in Eq.(116) into Eq.(117), expanding, and collecting terms in p gives

$$c_1 p^2 + c_2 p + c_3 = 0\,, \tag{118}$$

where

$$\begin{aligned} c_1 &= 2q_{23}C_2C_5 + q_{22}C_2^2 + q_{33}C_5^2 \\ c_2 &= 2\left[q_{12}C_2 + q_{13}C_5 + q_{23}\left(C_1C_5 + C_2C_4\right) + q_{22}C_1C_2 + q_{33}C_4C_5 \right] \\ c_3 &= q_{11} + 2\left(q_{12}C_1 + q_{13}C_4 + q_{23}C_1C_4\right) + q_{22}C_1^2 + q_{33}C_4^2 \quad . \end{aligned} \tag{119}$$

Eq.(119) is coded in subroutine **inter.F** as in.97–in.101. The quadratic expression in Eq.(118) is solved in subroutine **quad.F**. Real roots are used for POI plot analysis.

5.3. Intersection of two quadratics in the plot plane

The intersection of two quadratics in the plot plane makes use of Eq.(32) for both equations. The POI formulation yields a quartic polynomial. The analysis for the roots of a quartic has previously been developed (Cashwell and Everett, 1969) and the results are coded in subroutine **quart.F**. Real roots are used for POI plotting.

6. Geometry plotter coding implementations

The MCNP geometry plotter contains nine primary subroutines. A discussion and schematic of the code flow is presented in Appendix 2.

7. Summary and conclusions

The Los Alamos MCNP Monte Carlo code contains several useful features that were developed in the late 1970s to create and plot geometry for radiation-transport models. The MCNP geometry transformation capability permits the creation of objects using simple analytic geometry expressions and object translation and/or rotation to locations and/or orientations of interest in models. The geometry plotter provides 2-D images of slices through model geometry.

Until now, detailed derivations of the expressions used by MCNP to perform geometry transformations and geometry plots have not been available. Most of the equations underlying the MCNP geometry transformation and geometry plot utility have been derived here. Key expressions have been associated with lines of code in MCNPX (MCNPX contains line identifiers whereas MCNP does not). The derived equations agree with the expressions coded in MCNP.

The derivations indicate that the rotation-component "B" values in the *TRF* matrix are transposed in MCNP relative to the theoretical representation. Coded expressions in subroutines **trfsrf.F**, **dunlev.F**, etc. involving *TRF* matrix elements reflect this discrepancy. MCNP corrects for this by transposing the *TRF* rotation elements in subroutine **trfmat.F** during processing of the input data. Consequently, MCNP transposes the *TRF* matrix twice in order to perform the correct coordinate-

transformation operation. It is unclear why this treatment was coded in MCNP. Future work may be done to rewrite the code to simplify this treatment.

References

Breismeister J.F., ed., November 1993, "MCNP–A General Monte Carlo N–Particle Transport Code, Version 4A," Los Alamos National Laboratory report LA-12625-M, Ch. 2 pp. 159–161.

Brown F.B., ed., April 2003a, "MCNP–A General Monte Carlo N–Particle Transport Code, Version 5, Volume I: Overview and Theory," Los Alamos National Laboratory report LA-CP-03-0245, Ch 2 pp. 182–185.

Brown F.B., ed., April 2003b, "MCNP–A General Monte Carlo N–Particle Transport Code, Version 5, Volume II: User' Guide," Los Alamos National Laboratory report LA-CP-03-0245, Ch 3 pp. 31–32.

Cashwell E.D. and Everett C.J., December 1969, "Intersection of a Ray with a Surface of Third or Fourth Degree," Los Alamos Scientific Laboratory report LA-4299.

Hsiung C.Y. and Mao G.Y., 1998, *Linear Algebra*, World Scientific, New Jersey, pp. 141–172.

Kwak J.H. and Hong S., 1997, *Linear Algebra*, Birkhauser, Boston, pp. 279–291.

Pelowitz D.B., ed., April 2011, "MCNPX User's Manual Version 2.7.0," Los Alamos National Laboratory report LA-CP-11-00438.

Spain B., 2007, *Analytical Conics*, Dover Publications, Inc., Mineola, NY, pp. 66–70.

Thompson W.L., ed., November 1979, "MCNP–A General Monte Carlo Code for Neutron and Photon Transport," Los Alamos National Laboratory report LA-7396-M, Revised, pp. 111–114.

Thompson W.L., Cashwell E.D., Godfrey T.N.K., Schrandt R.G., Deutsch O.L., and Booth T.E., May 1980, "The Status of Monte Carlo at Los Alamos," Los Alamos National Laboratory report LA-8353-MS, pp. 17–22.

Thompson W.L., ed., November 1981, "MCNP–A General Monte Carlo Code for Neutron and Photon Transport, Version 2B" Los Alamos National Laboratory report LA-7396-M, Revised, p.1.

Tierney J.A., 1974, *Calculus and Analytic Geometry*, Allyn and Bacon, Inc., Boston, p. 226.

Trench W.F. and Kolman B., 1972, *Multivariable Calculus with Linear Algebra and Series*, Academic Press, Inc., New York, pp. 222–223.

Wolfram S. (1991), *Mathematica*, Addison-Wesley, New York, Second Edition, pp. 121–124.

Wylie C.R. (1975), *Advanced Engineering Mathematics*, McGraw-Hill, New York, pp. 636–637.

APPENDIX 1

The geometry portion of the input file for the test problem presented in Section 5 is listed below.

```
Boxes to illustrate geometry plots.
c
c boxes & outer sphere
1   0   #2 #3 -1                    $outer sphere containing 2 boxes
2   0   10 -11  12 -13  14 -15      $upper box
3   0   20 -21  22 -23  24 -25      $lower box
c outside
100 0          1

c  surfaces
   1 so  5.0          $sphere of radius 5.0 centered at the origin
c  upper box
   10 px -2.5         $plane at x=-2.5
   11 px -0.5         $plane at x=-0.5
   12 py  1.0         $plane at y= 1
   13 py  3.0         $plane at y= 3
   14 pz -1.0         $plane at z=-1
   15 pz  1.0         $plane at z= 1
c  lower box
   20 px  0.5         $plane at x= 0.5
   21 px  2.5         $plane at x= 2.5
   22 py -3.0         $plane at y=-3
   23 py -1.0         $plane at y=-1
   24 pz -1.0         $plane at z=-1
   25 pz  1.0         $plane at z= 1
```

APPENDIX 2

The MCNP geometry plotter makes use of nine primary subroutines. An overview of these subroutines is provided here.[†]

As illustrated in Fig. 8, MCNP execution begins with the **main.F**, which controls initialization, plotting, cross-section input, and particle transport. Subroutine **imcn.F** is called by **main.F** to initiate transport. Subroutine **imcn.F** calls **igeom.F** where the problem geometry is set up using subroutines **mbody.F**, **trfsrf.F**, and **amatrx.F**. Subroutine **mbody.F** changes the macrobody representation of surface coefficients into simple surfaces. Subroutine **trfsrf.F** is then used to perform any need transformations of surfaces from local to global coordinates. Subroutine **trfsrf.F** uses **amatrx.F** to change surface-coefficient representations from general quadratic to matrix form as discussed in the material related to Eqs.(1)–(9). Following initialization, **plotg.F** is called for geometry plotting.

[†] Original versions of several of these subroutines are identified in mcnp1a, release date August, 1977, as having been created by Charles A. Forest late in 1974 at Los Alamos Scientific Laboratory. Revisions to these subroutines have been made since mcnp1a.

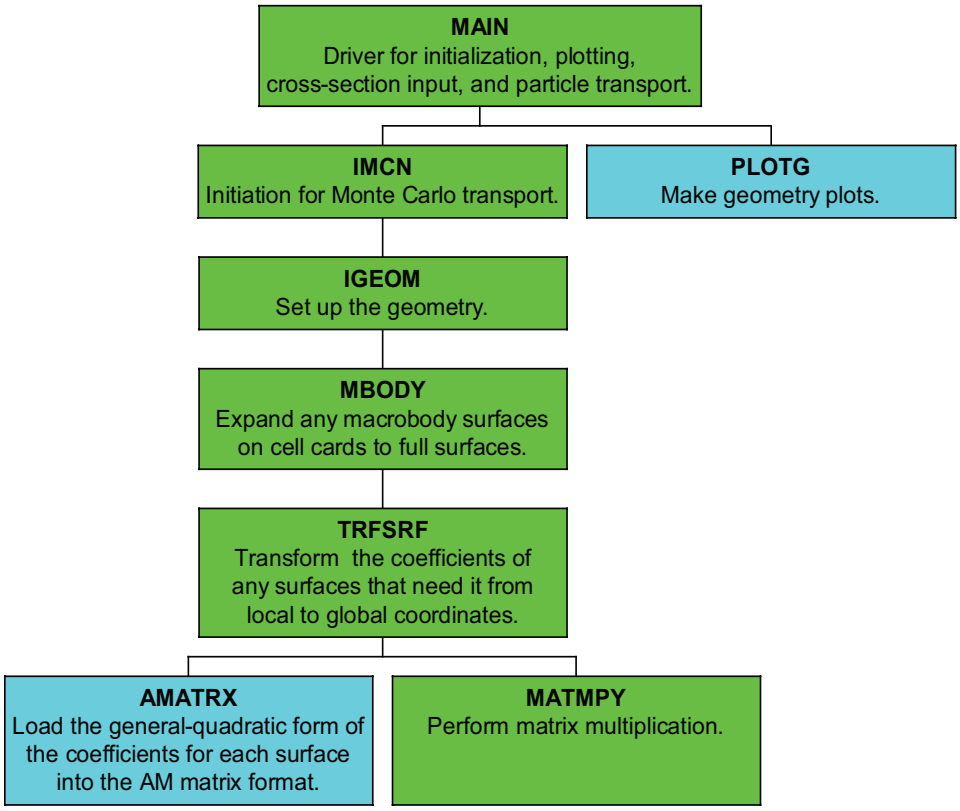

Figure 8. Initialization aspect of geometry plotting using MCNP. The primary subroutines used for geometry plotting are shown in the blue boxes.

Ash sown in Fig. 9, subroutine plotg.F calls two principal subroutines, **amatrx.F** and **viewz.F**. Subroutine **amatrx.F** loads the general-quadratic form of the surface coefficients for each surface into matrix form. At this point in execution, these coefficients are the global-coordinate values AM^G as given in Eq.(9).

Subroutine **viewz.F** is the driver routine for the calculation of the arcs and cell number locations to be plotted. For each surface, **viewz.F** calls **regula.F** and **pltsrf.F** to calculate the points that define the arcs used to plot each portion of each surface. Code flow for these subroutines is shown in Fig. 9.

Subroutine **regula.F** calculates several quantities. First, the QM matrix coefficients for each surface are calculated as discussed in the material related to Eqs.(25)–(32). Second, the coefficients for the univariate equations in p are calculated for each arc. If the QM coefficients are such that the equation is a straight line, the constants in Eq.(70) are calculated directly. The diagonalization procedure discussed in the material related to Eqs.(34)–(42) and Sections 4.2 and 4.3 is used for parallel or intersecting lines, a parabola, ellipse, or hyperbola. For this procedure the diagonalization parameters θ^D, s_0, and t_0 parameters in Eqs.(45), (82), and (83) and the translation-rotation DIA in Eq.(36) are calculated. The QM matrix is then formed using Eq.(39) to give the quadratic form given of the curve in u,v in Eq.(43). The quadratic coefficients are evaluated to determine whether the type of curve(s): parallel or intersecting lines, a parabola, ellipse, or hyperbola. Finally, the coefficients for the univariate equations in p are calculated. For an ellipse, circle, or point, the coefficients (square-root quantities) in Eq.(86) are used; for a hyperbola the coefficients in Eq.(97) are used, and for a parabola the constants in Eqs.(104) or (109) are used.

Subroutine **pltsrf.F** is the driver for the calculation of the points that define each of the arcs of each surface in the plot plane. Points defining each are are loaded into a buffer for plotting.

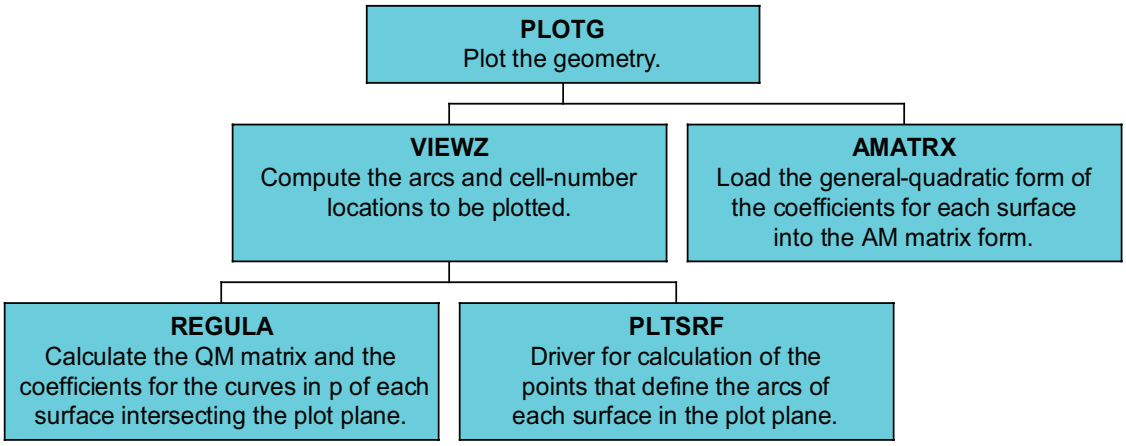

Figure 9. MCNP upper-level geometry plotting subroutines.

Figures 10 and 11 show the subroutines associated with **pltsrf.F**. Subroutine **pltsrf.F** calls **inter.F**, **ptost.F**, and **chkcel.F**. Subroutine **inter.F** is used to find the intersections within the plot window of each curve with all other curves. To do so, **inter.F** uses **sstop.F** to determine the points where each curve (straight line, parabola, ellipse, hyperbola) crosses the window boundary and **regula.F**. The POI for the intersection of two lines, as given in Eq.(114), is calculated in **inter.F**. For the intersection of a line and a general quadratic in the plot plane, subroutine **inter.F** calls **quad.F** to solve Eq.(118) using Eq.(119) for one or two POIs. The intersection of two quadratics yields a quartic polynomial that is solved using subroutine **quart.F** for the POIs.

Subroutine **ptost.F** calculates the point $s(p), t(p)$ from the parametric representation of each curve in the plot plane. Expressions for a straight line, parabola, ellipse, and hyperbola are given in Eqs.(69)–(70), (103)–(104), (88)–(89), and (96)–(97), respectively.

Subroutine **chkcel.F** is used to check the sense of a point on either side of an arc to identify the cells on either side of the arc. This information is used to set the type of line to be plotted for each segment of the curve. When the geometry is well defined either 1) no line is plotted when there are identical cells on either side of the curve or 2) a solid line is plotted when different cells are located on opposite sides of the curve. When the geometry is erroneous, a dashed line is plotted.

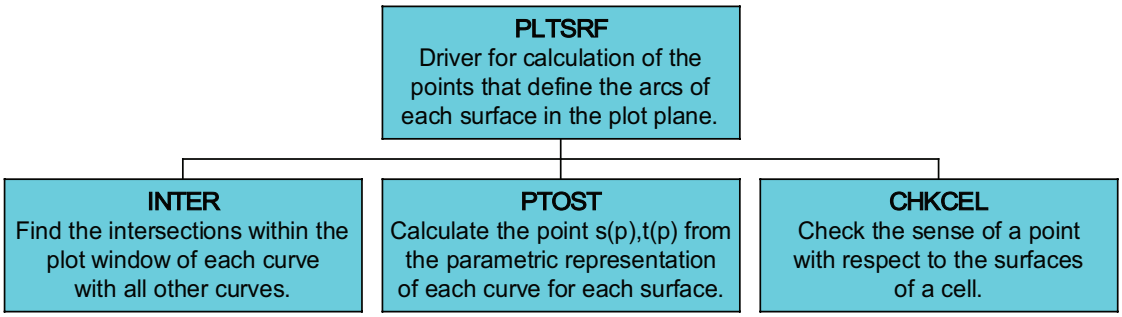

Figure 10. MCNP lower-level geometry plotting subroutines associated with **pltsrf.F**.

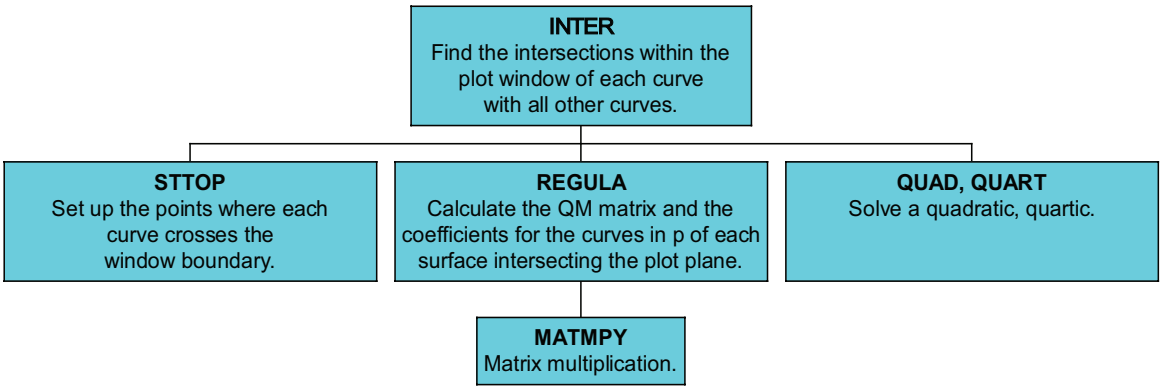

Figure 11. MCNP lower-level geometry plotting subroutines associated with **inter.F**.

List of Figures

Figure 1. General geometry transformation and plotting code flow for geometry transformation.

Figure 2. Coordinate-system rotation illustrated by global and local rectangular coordinate systems having the same origin.

Figure 3. Plot plane and rectangular object.

Figure 4. Geometry plot for the correct model.

Figure 5. Geometry plot for error created by omitting #3 in the description of cell 1.

Figure 6. Geometry plot for error created by incorrectly specifying surface 23 of cell 3 with a positive sense.

Figure 7. Geometry plot displaying errors created by incorrectly specifying surface 23 of cell 3 and surface 11 of cell 2 as having a positive sense.

Figure 8. Initialization aspect of geometry plotting using MCNP. The primary subroutines used for geometry plotting are shown in the blue boxes.

Figure 9. MCNP upper-level geometry plotting subroutines.

Figure 10. MCNP lower-level geometry plotting subroutines associated with **pltsrf.F**.

Figure 11. MCNP lower-level geometry plotting subroutines associated with **inter.F**.

List of Tables

None.